



# Contrasting Dynamic Behaviour of Five Lake-terminating Glaciers Draining the Vatnajökull Ice Cap and Links to Bedrock Topography

Nathaniel R. Baurley<sup>1</sup> · Amelia Andrews<sup>1</sup> · Benjamin Robson<sup>2</sup> · Sherif Attia<sup>3</sup> · Kirk Martinez<sup>3</sup> · Jane K. Hart<sup>1</sup>

Received: 26 August 2024 / Revised: 10 January 2025 / Accepted: 6 March 2025 / Published online: 1 April 2025  
© The Author(s) 2025

## Abstract

Over recent years, the rapid growth and development of proglacial lakes at the margin of many of Iceland's outlet glaciers has resulted in heightened rates of mass loss and terminus retreat, yet the key processes forcing their dynamic behaviour remain uncertain, particularly at those glaciers which are underlain by overdeepened bedrock troughs. As such, we utilised satellite remote sensing to investigate the recent dynamic changes at five lake-terminating glaciers draining the Vatnajökull ice cap. Specifically, we quantified variations in surface velocity between ~2008–2020, alongside datasets of frontal retreat, proglacial lake growth, bedrock topography and ice surface elevation change to better understand their recent dynamics and how this may evolve in future. We observed contrasting dynamic behaviour between the five study glaciers, with three displaying a heightened dynamic response (Breiðamerkurjökull, Fjallsjökull, Skaftafellsjökull), which was likely driven by retreat down a reverse-sloping bed into deeper water and the onset of dynamic thinning. Conversely, one glacier re-advanced (Kvíárjökull), whilst the other remained relatively stable (Svínafellsjökull), despite the presence of overdeepened bedrock troughs under both these glaciers, highlighting the complex nature of those processes that are driving the dynamic behaviour of lake-terminating glaciers in this region. These findings may be important in helping understand the processes driving the dynamics of other lake-terminating glaciers in Iceland so that their future patterns of retreat and mass loss can be more accurately quantified.

**Keywords** Glacier dynamics · Glacier velocity · Proglacial lakes · Glacier retreat · Glacier calving · Remote sensing · Glacier monitoring

## 1 Introduction

Glaciers are highly sensitive to climate change, with widespread glacier retreat forecast to continue as global climate warming intensifies [1–3]. This has important implications for their meltwater contribution to global sea level rise (SLR) [4–6], as well as for regional hydrology due to the strong control glacier meltwater has on modulating down-glacier streamflow. This in turn affects freshwater availability, hydropower operations and sediment transport [2, 7, 8].

Detailed glacier monitoring is, therefore, required, so that future patterns of glacier retreat and mass loss can be more accurately quantified [5, 7, 9].

In recent years, there has been growing interest in the glaciers and ice caps of Iceland, due in part to their high sensitivity to atmospheric warming, but also because they contain a disproportionately large amount of Europe's freshwater resources (and thus SLR contribution) [10–12]. Indeed, like many glaciers and ice caps globally, Iceland's ice masses have been losing mass since the Little Ice Age (~1890) [10, 13]. However, in recent decades the rate of mass loss has accelerated, with nearly half of the total mass loss since the Little Ice Age having occurred since 1994 [14]. Such a response can be attributed to the recent rapid warming of the Arctic, as well a shift in atmospheric and oceanic circulation patterns around Iceland [10, 15]. This resulted in  $\sim 240 \pm 20$  Gt of mass loss for the period 1994–95 to 2018–19 ( $9.6 \pm 0.8$  Gt  $a^{-1}$ ) [14], with the most rapid mass loss ( $11.6 \pm 0.8$  Gt  $a^{-1}$ ) occurring between 2003–2010 [13].

✉ Nathaniel R. Baurley  
n.baurley@soton.ac.uk

<sup>1</sup> Geography and Environmental Science, University of Southampton, Southampton, UK

<sup>2</sup> Department of Earth Science, University of Bergen, Bergen, Norway

<sup>3</sup> Electronics and Computer Science, University of Southampton, Southampton, UK

However, while the overall trend is one of increasing mass loss, there is significant interannual variability [13]. For example, as a result of regional cooling in the North Atlantic, the mass loss rate has on average been 50% lower since 2010 [12], yet 2018–19 was one of the most negative mass balance years on record ( $-15 \pm 1.6 \text{ Gt a}^{-1}$ ) [14]. Furthermore, recent research has shown that non-surface mass balance processes, such as geothermal melting, volcanic eruptions, and frontal ablation, have also contributed significantly to the recent patterns of mass loss (e.g., [16–18]). Indeed, these processes are thought to account for ~20% of the total mass loss since 1994, whilst at some ice caps, including the southern part of Vatnajökull, they account for nearly 40% [14, 17].

Of these processes, one of the most important is frontal ablation (i.e., glacier calving), which can decouple the dynamic behaviour of a glacier from a climate, resulting in accelerated terminus retreat and mass loss [19–21]. Although the influence of calving was insignificant during the first half of the 20<sup>th</sup> century, its contribution to mass loss has gradually increased since the mid-1990s in response to the ongoing retreat of outlet glaciers through overdeepened bedrock troughs [14, 22]. For example, many of the southerly-flowing outlets of the country's largest ice cap, Vatnajökull, are underlain by deep bedrock troughs, including Svínafellsjökull (320 m), Breiðamerkurjökull (300 m) and Hoffellsjökull (> 250 m) [22, 23]. This has led to the rapid development and expansion of proglacial lakes at the margins of these glaciers and consequently, the onset of calving, resulting in accelerated terminus retreat and mass loss [24, 25]. Importantly, such patterns of proglacial lake expansion, retreat, and mass loss are forecast to continue in future, with significant implications for glacier dynamics in the region [17, 26].

Of these southern outlets, it is the dynamic behaviour of Breiðamerkurjökull which has received the most attention in the literature over the last decade (e.g. [26–29]), although these studies have tended to only focus on those small-scale changes occurring over short time scales (e.g. [27]), or on one aspect of its dynamic behaviour (e.g. [29]). Most recently, however, Baurley et al. [30] utilised satellite remote sensing to investigate the changing dynamics of the glacier over a 27-year period. The authors attribute the recent increase in velocities and retreat of the glacier to the increase in size and depth of its proglacial lake Jökulsárlón, as the glacier retreated into the 200–300 m deep bedrock trough it formed during the Little Ice Age. The authors suggest that while initial retreat was instigated by rising air temperatures, once Jökulsárlón increased to a sufficient size where it was able to start influencing frontal retreat and ice flow, then this became the dominant mechanism in causing the rapid retreat, thinning and flow

velocities observed since the turn of the twenty-first century [30].

In contrast, the dynamic behaviour of many of the other southerly-flowing outlets of Vatnajökull have received comparatively little focus, despite several of these outlets also having basal troughs some 200–300 m below sea level [22, 23]. Indeed, while the dynamics of Fjallsjökull, the neighbouring glacier to Breiðamerkurjökull, has received growing interest over the last few years (e.g., [24, 31, 32]), the recent dynamic behaviour of the remaining outlets remains poorly understood. In particular, those studies which investigate the different drivers of these changes over extended time periods, such as the studies of Dell et al. [24] and Baurley et al. [30], are lacking. As a result, further research across extended spatial (e.g., regional) and temporal (e.g., decadal) scales are required to put these dynamic changes into context so that the future patterns of retreat and mass loss, and subsequently the SLR contribution, of these rapidly changing lake-terminating glaciers can be more accurately quantified.

Therefore, this study aims to investigate the recent dynamic changes at five lake-terminating glaciers draining the Vatnajökull ice cap. More specifically, we use high-resolution satellite imagery to quantify variations in surface velocity from ~2008–2020, alongside datasets of frontal retreat, proglacial lake growth, bedrock topography and ice surface elevation change to better understand their dynamic behaviour and how this may evolve in future. For the first two glaciers (Breiðamerkurjökull and Fjallsjökull), we extend the record previously described by Baurley et al. [30] and Dell et al. [24], respectively, in order to assess their ongoing dynamic evolution. For the third glacier (Kvíárjökull), we further develop the recent work of Kavan et al. [11] to provide new insights into its dynamic behaviour, whilst at the final two glaciers (Svínafellsjökull and Skaftafellsjökull) we provide the very first insights into their recent velocity patterns and overall dynamics. We believe our findings from these sites may be used to better understand and predict how other, similar lake-terminating glaciers in Iceland, as well as in Alaska, the Himalaya, and Scandinavia, may respond to both future warming and calving dynamics.

## 2 Study Site

The five outlet glaciers of interest in this study are all located on the southern slopes of the Vatnajökull Ice Cap, in southwest Iceland (Fig. 1). Breiðamerkurjökull, the largest of the five glaciers (906 km<sup>2</sup> in 2010), is composed of four main lobes, or 'arms', separated by three large medial moraines (Fig. 1C) [29, 33]. The larger, eastern arm drains the ice dome of Breiðabunga deep within the ice cap [34]. The central arm flows out from the two large nunataks Máfabýggðir (1440 m a.s.l.) and Esjufjöll

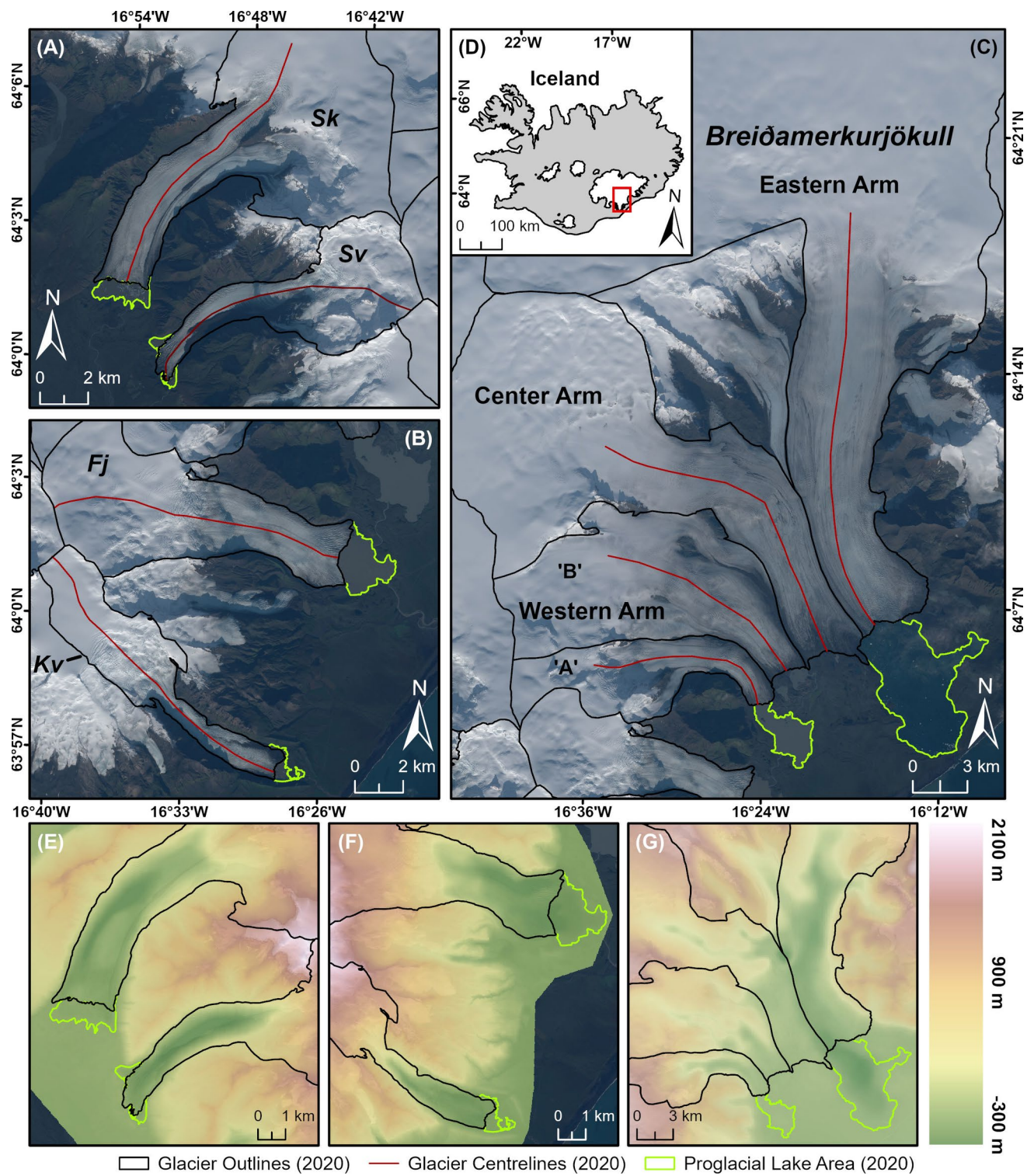


**Fig. 1** Area of (A) Skaftafellsjökull (Sk) and Svínafellsjökull (Sv), (B) Fjallsjökull (Fj) and Kvíárjökull (Kv) and (C) Breiðamerkurjökull, as of 2020. (D) Location of the five study glaciers within Iceland. Glacier outlines obtained from the GLIMS database. Centrelines derived manually using the geometry of the outlines. (E) Bedrock topography of Skaftafellsjökull and Svínafellsjökull, and

(F) Fjallsjökull and Kvíárjökull, interpolated from contours provided to the authors by E. Magnússon. (G) Bedrock topography of Breiðamerkurjökull interpolated from contours provided in Björnsson [35]. Background image is a Sentinel-2 acquisition (3, 2, 1 RGB) from 13/10/2020

(1770 m a.s.l.) (Guðmundsson and Björnsson, 2016), whilst the two western arms, Western A and Western B (after [30]), drain the north-eastern flank of the Örafajökull Ice Cap, which itself is situated on the southern slopes of Vatnajökull, and is the highest peak in Iceland (~ 2000 m a.s.l.).

Two lakes of contrasting sizes are also present at the glacier terminus: the large, ~ 27 km<sup>2</sup> Jökulsárlón, adjacent to the eastern arm, and the smaller ~ 5.8 km<sup>2</sup> Breiðárlón, adjacent to Western A (Fig. 1C) [30]. Most of the glacier bed sits at, or just above, sea level (10–100 m a.s.l.), however a small, shallow trough extends back from the margin of Western A, while a large, ~ 300 m deep trough is found under Jökulsárlón, which extends ~ 20 km up-glacier into the interior (Fig. 1G) [22]. It was demonstrated by Baurley et al. [30] that the central and Western B arms of Breiðamerkurjökull have undergone very little change in their dynamics over recent decades [30]. As such, in this study we will focus on the lake-terminating eastern and Western A arms of the glacier due to their highly dynamic and rapidly changing nature.

Fjallsjökull and Kvíárjökull (44.6 km<sup>2</sup> and 23.2 km<sup>2</sup> in 2010, respectively), are located on the steep, eastern and south-eastern slopes of the Örafajökull Ice Cap (Fig. 1B) [25]. Both glaciers descend rapidly over a series of ice falls before terminating at low elevation (~ 30 m a.s.l.) in their respective proglacial lakes: the 3.7 km<sup>2</sup> Fjallsárlón (at Fjallsjökull), and the 0.6 km<sup>2</sup> Kvíárjökulsón (at Kvíárjökull) [22]. Both glaciers are also underlain by relatively deep bedrock troughs, with a ~ 200 m deep trough under Fjallsjökull and a ~ 100 m deep trough under Kvíárjökull (Fig. 1F) [24, 25].

In contrast, Svínafellsjökull and Skaftafellsjökull (33.2 km<sup>2</sup> and 84.1 km<sup>2</sup> in 2010, respectively), are situated on the steep western, and north-western slopes of Örafajökull (Fig. 1A) [25]. Both glaciers again descend to low elevation (~ 100 m a.s.l.) before terminating in unnamed proglacial lakes: the ~ 0.4 km<sup>2</sup> lake at Svínafellsjökull (comprising a separate northern and southern lake), and the ~ 1.3 km<sup>2</sup> lake at Skaftafellsjökull [22]. Particularly deep bedrock troughs are again found under these glaciers, with a ~ 300 m deep trough under Svínafellsjökull and ~ 200 m deep trough under Skaftafellsjökull (Fig. 1E) [22, 25].

In addition, data from the nearby meteorological station at Fagurhólmsmýri (63°52' N, 16°38' W), which is located ~ 4 km away at an elevation of ~ 16 m a.s.l., indicates that this region of Iceland has undergone a 1.5 °C increase in mean annual air temperatures since ~ 1980. Yet despite this, previous research has shown that deep proglacial lakes can exert a significant influence on the overall dynamics and retreat patterns of the glaciers that terminate in them (e.g., [24, 30]), and thus further research into the processes currently underway at these lake-terminating glaciers is

warranted in order to better understand their likely future response.

### 3 Material and Methods

In this study, glacier velocity, as well as variations in ice front position and proglacial lake area, were measured using satellite imagery for the period 2008–2020 for Breiðamerkurjökull and Fjallsjökull, and 2010–2020 for Kvíárjökull, Svínafellsjökull and Skaftafellsjökull (Table S1). Glacier-wide velocities were assessed using TerraSAR-X imagery, acquired in strip-map mode with a resolution of 2 m and HH polarisation. Ice-front position and variations in proglacial lake area were assessed using orthorectified optical images from the Landsat 7 ETM+ and 8 OLI/TIRS satellites (panchromatic band, 15 m resolution) and the Sentinel-2 constellation (10 m resolution). Where possible, data acquired in late-summer (August–October) were downloaded to allow direct comparisons to be made between years (Table S2, S3). However, this was not always possible due to data availability, as well as the presence of cloud cover which impacted the usability of the optical imagery, so in these instances the next nearest usable dates were selected.

#### 3.1 Glacier-wide Velocities

Velocity data were generated using the offset tracking algorithm within the European Space Agency (ESA) Sentinel Application Platform (SNAP). Offset tracking estimates the movement of glacier surfaces between master and slave images in both the slant-range and azimuth-direction through cross-correlation on selected ground control points [36–38]. The movement velocity is then computed based on the offsets estimated by the cross-correlation algorithm, with these values then interpolated to create a map of glacier velocity [30, 39]. The method is particularly advantageous because it is less sensitive to loss of coherence between images, and as such it is widely used in glacier motion assessment (e.g., [38–40]).

Here, each pair of SAR images were first calibrated and then co-registered using the aerial LiDAR DEM of Iceland, provided at a resolution of 10 m by the National Land Survey of Iceland [41]. Velocities were then calculated using cross correlation, with specific parameters, including the moving window size and search distance, varying between each specific glacier (Table S4). Any displacements with a cross-correlation threshold of < 0.01 were then removed, with the remaining displacements averaged over a mean pixel grid and converted to ground range coordinates, resulting in velocity rasters at 2 m resolution. To allow for a more-robust comparison of the velocity data between individual

years, we present mean velocity measurements taken at 1 km intervals along the glacier centrelines (shown in Fig. 1), after Baurley et al. [30].

The stochastic error in our velocity measurements was assessed by measuring displacements over terrain that we regarded as stable (Figure S1) [30, 42]. The average RMSE for all five glaciers over the entire period was  $\pm 0.09 \text{ m d}^{-1}$ . More specifically, the average RMSE for Breiðamerkurjökull was  $\pm 0.10 \text{ m d}^{-1}$ , while for the other four glaciers it was  $\pm 0.09 \text{ m d}^{-1}$ , indicating that our estimated levels of uncertainty are not greater than the change in velocity observed over the duration of our study.

### 3.2 Frontal Position and Lake Area Change

Variations in ice-front position were assessed by manually digitising the terminus of each glacier at different time steps using a combination of Landsat 7 & 8, and Sentinel-2, optical imagery. The frontal position of both the eastern and Western A arms of Breiðamerkurjökull, as well as Fjallsjökull, were digitised at six time-steps between 2008 and 2020, whilst the front positions of Kvíárjökull, Svínafellsjökull and Skaftafellsjökull were digitised at five time-steps between 2010 and 2020. All frontal positions were digitised at a scale of 1:10,000, which ensured each position could be accurately mapped, and prevented pixelated images hindering reliable interpretation (e.g., [24]).

The rectilinear box method was then used to calculate the positional change through time for each glacier and time step of interest (e.g., [43]). The method was employed here due to its ability to account for asymmetric changes at the calving front (e.g., [24, 44, 45]). When calculating the positional change occurring at the calving front of the Eastern and Western A arms of Breiðamerkurjökull, the width of the box only encompassed the maximum delineated width of the lake terminating portion of the front, rather than the whole terminus of both arms. This ensured that the captured rate of positional change actively related to what was occurring at the calving front.

Changes in lake area were assessed using the same imagery, time steps and digitising scale used to quantify frontal position change, with the area of each proglacial lake manually digitised at each time step. Channels exiting each of the lakes were ignored during digitisation at the point where the channel began to form.

To quantify the uncertainty of the manual digitising procedure, the area of each proglacial lake in 2012, 2014 and 2020 were repeatedly digitised 10 times at the same scale used in the original analyses, before calculating the standard error [30]. For all proglacial lakes, the RMSE was  $< 1\%$  of the original measured value (Table S5), indicating that the calculated uncertainty was not greater than the change observed over the duration of our study.

### 3.3 Ice Surface Elevation Change

Changes in ice surface elevation were evaluated using the freely available global ice surface elevation change dataset compiled by Hugonnet et al. [5] (available at <https://doi.org/10.6096/13>). The dataset provides elevation change rasters at 100 m resolution, alongside their 1-sigma uncertainty, for all glaciated regions on earth at different temporal extents. For this study, elevation change rasters covering each of the five glaciers were downloaded for the period 2010–2019, enabling us to assess how the surface of each glacier has changed across almost the entirety of our study period, as well as the potential drivers of this change. The 1-sigma uncertainty values, which had been aggregated for each study glacier, were then used to estimate the uncertainty of the observed changes in ice elevation. This provided a greater degree of confidence that the visualised changes in ice surface elevation represented actual change.

## 4 Results

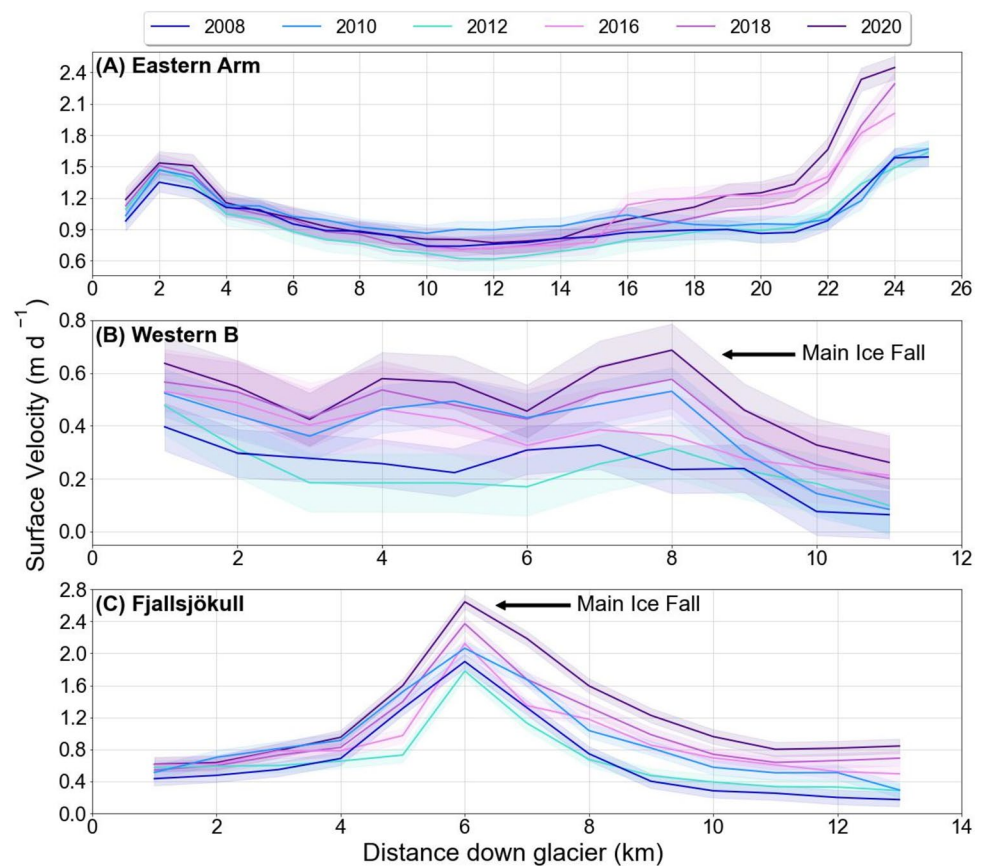
### 4.1 Glacier-wide Velocities

We observe spatially variable velocity change for all five study glaciers across the period 2008/2010–2020. In general, all glaciers see an increase in velocity over this period, although there is distinct variability in the velocity patterns exhibited by each individual glacier in each year. These patterns are visualised in the mean centreline velocities for each glacier (Figs. 2 and 3), as well as the annual velocity (Figures S2–S4) and velocity change rasters (Figure S5), with key variations described below.

At Breiðamerkurjökull, there is a distinct contrast in the velocity pattern displayed by the larger, more dynamic eastern arm and the other three arms of the glacier, with the highest velocities consistently observed at the eastern arm over the study period. Overall, velocities increase down-glacier, with a particularly rapid increase in velocity observed in the near-terminus region, within  $\sim 3\text{--}4 \text{ km}$  of the calving front (Fig. 2A, S2, S5C). In this region, mean velocities increase from  $\sim 1.59 \pm 0.10 \text{ m d}^{-1}$  in 2008 to  $\sim 2.45 \pm 0.10 \text{ m d}^{-1}$  in 2020 ( $\sim 54\%$  increase) (Fig. 2A), with nearly half of this increase ( $\sim 22\%$ ) occurring between 2016–2020.

In contrast, comparatively low velocities are observed at Western A over the same period, with these tending to decrease (rather than increase) down-glacier (Figure S2). However, velocities do also increase over the study period (Figure S5C). For example, velocities over the main ice fall increase from  $\sim 0.24$  to  $\sim 0.69 \pm 0.10 \text{ m d}^{-1}$  (188% increase), whilst mean near-terminus velocities increase significantly from  $\sim 0.06$  to  $\sim 0.26 \pm 0.10 \text{ m d}^{-1}$  (333% increase) (Fig. 2B).

**Fig. 2** Velocity profiles for the (A) Eastern and (B) Western A arms of Breiðamerkurjökull, as well as (C) Fjallsjökull, for the period 2008–2020, calculated by taking the mean velocity at 1 km intervals along the centrelines shown in Fig. 1B & C. Associated uncertainty margins for each year are also shown (note the difference in scale)



At Fjallsjökull, velocities also decrease down-glacier, with the fastest velocities again observed over the main ice fall in all years (Figure S3, S5B). Indeed, mean velocities in this region increase from  $\sim 1.89 \pm 0.09 \text{ m d}^{-1}$  in 2008 to  $2.65 \pm 0.09 \text{ m d}^{-1}$  in 2020 (40% increase), with over half of this increase ( $\sim 25\%$ ) occurring since 2016 (Fig. 2C). However, and akin to the pattern observed at Western A, mean near-terminus velocities also increase significantly during this time, from  $\sim 0.14$  to  $0.82 \pm 0.09 \text{ m d}^{-1}$  ( $\sim 485\%$  increase) (Fig. 2C, S5B). Furthermore, from 2018 onwards, velocities in the near-terminus region (within  $\sim 2$  km of the front) begin to increase up to the calving front, rather than decrease (Fig. 2C). This is similar to the pattern observed at the eastern arm of Breiðamerkurjökull over 2008–2020.

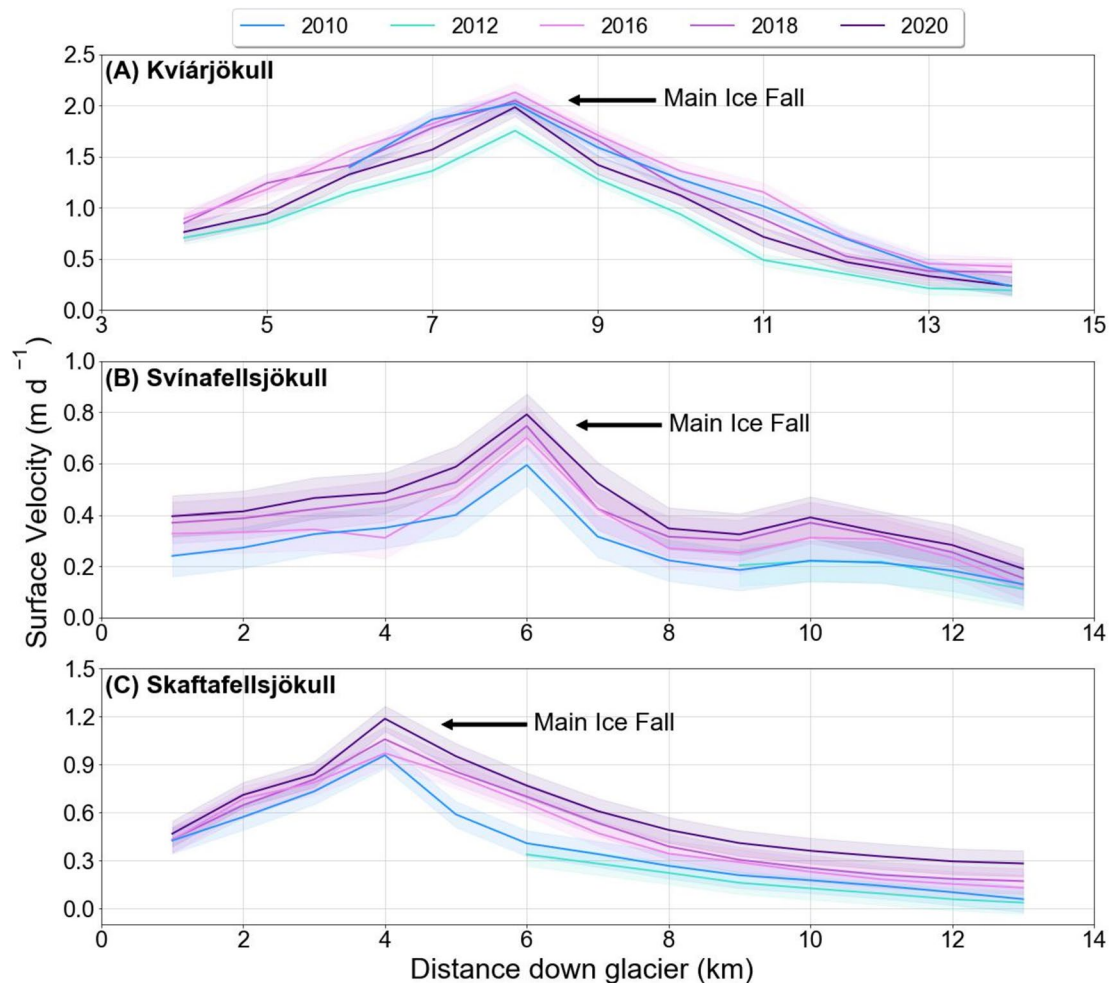
In general, velocities at Kvíárjökull display a similar pattern to those observed at Fjallsjökull over the same period, with velocities decreasing down-glacier and the fastest velocities observed over the main ice fall (Figure S3, S5B). However, mean near-terminus velocities peak in 2016, increasing from  $\sim 0.19 \pm 0.09 \text{ m d}^{-1}$  in 2012 to  $0.42 \pm 0.09 \text{ m d}^{-1}$  (121% increase) (Fig. 3A). Velocities in this region then decrease up to the end of the study period, so that by 2020 velocities are a similar magnitude to those observed in 2010, with a similar pattern observed over the main ice fall. This is

the only glacier in our study where near-terminus velocities do not peak at the end of the study period (i.e., in 2020).

Lastly, velocities at both Svínafellsjökull and Skafafellsjökull display a similar pattern to those observed at Fjallsjökull over the study period, with velocities decreasing down-glacier, and the fastest velocities once again observed over the main ice fall of both glaciers (Figure S4, S5A). Mean near-terminus velocities also increase during this time, although the magnitude of the observed velocity change differs between the two glaciers. At Svínafellsjökull, velocities over the main ice fall increase by  $\sim 33\%$  over the study period, whilst mean near-terminus velocities gradually increase from  $\sim 0.12$  to  $0.19 \pm 0.09 \text{ m d}^{-1}$  (58% increase) (Fig. 3B). In contrast, while velocities over the main ice fall of Skafafellsjökull increase by  $\sim 25\%$  over the study period, mean near-terminus velocities increase by almost 500%, from  $\sim 0.05$  to  $\sim 0.30 \pm 0.09 \text{ m d}^{-1}$  (Fig. 3C). This is significantly greater than the velocity increase observed at Svínafellsjökull over the same period.

#### 4.2 Frontal Position and Lake Area Change

In general, all five glaciers retreated over the study period, whilst the area of their proglacial lakes increased, with the rate at which these changes occurred varying considerably



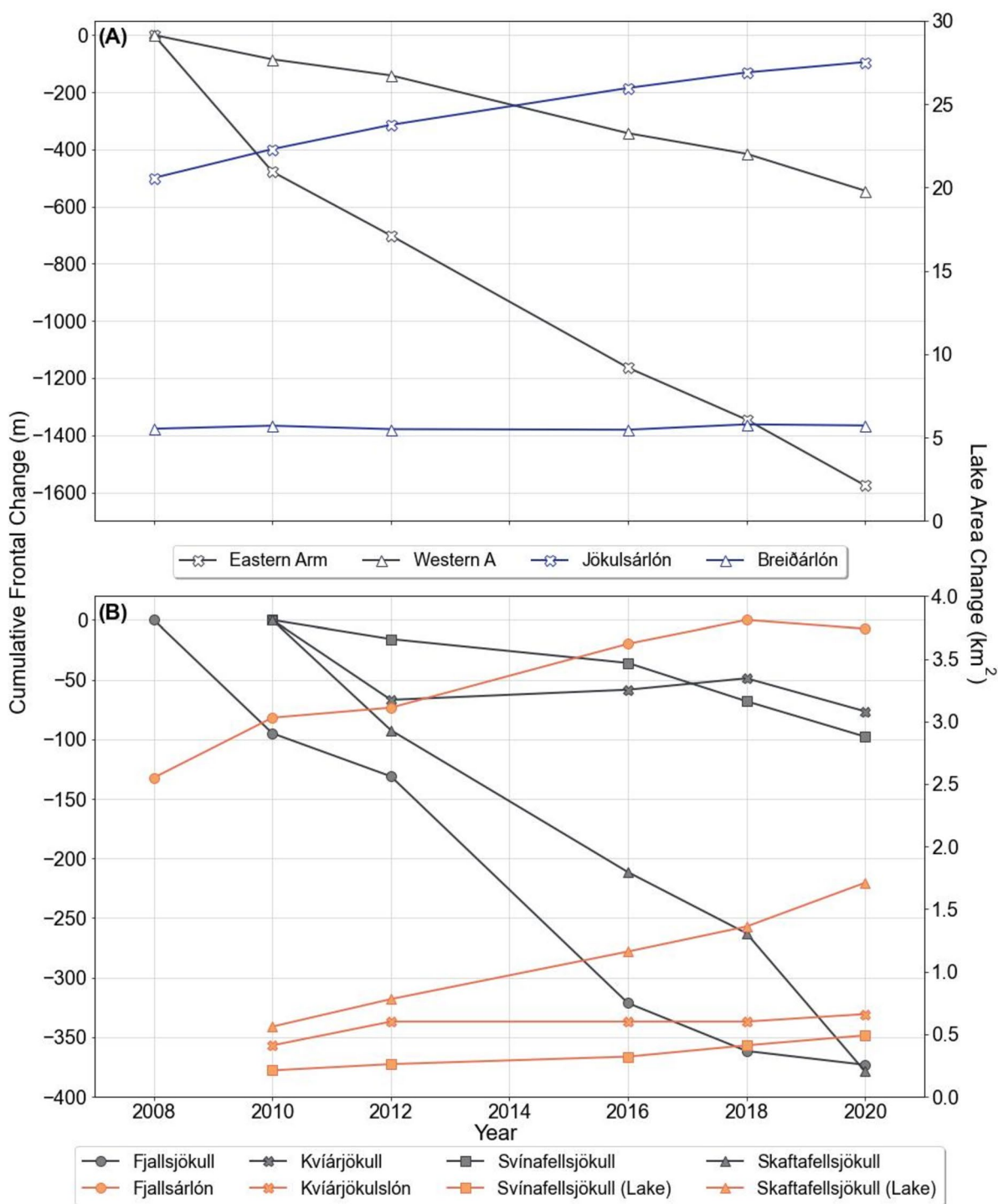
**Fig. 3** Velocity profiles for (A) Kvíárjökull (B) Svínafellsjökull and (C) Skaftafellsjökull for the period 2010–2020, calculated by taking the mean velocity at 1 km intervals along the centrelines shown in

Fig. 1A & B. Associated uncertainty margins for each year are also shown (note the difference in scale)

between the individual glaciers (Fig. 4, S6, S7). The greatest change in frontal position is observed at the eastern arm of Breiðamerkurjökull, which retreated by nearly 1600 m between 2008–2020, at a rate of  $\sim 131.29 \text{ m a}^{-1}$  (Fig. 4A, S6A). Over the same period, the area of its proglacial lake, Jökulsárlón, increased by  $\sim 34\%$ , from 20.57 to 27.52  $\text{km}^2$ , equating to growth rate of  $0.58 \text{ km}^2 \text{ a}^{-1}$  (Fig. 4A). This is both the largest increase in proglacial lake area and the fastest rate of proglacial lake growth observed in this study (Figure S7A).

In contrast, the other lake-terminating arm of the glacier, Western A, retreated by  $\sim 540 \text{ m}$  (rate of  $\sim 45.39 \text{ m a}^{-1}$ ), whilst its proglacial lake, Breiðárlón, grew marginally by  $\sim 4\%$  from 5.53 to 5.73  $\text{km}^2$  (growth rate of  $\sim 0.02 \text{ km}^2 \text{ a}^{-1}$ ) (Fig. 4A). This represents both the smallest change in proglacial lake area and the slowest rate of proglacial lake growth that we observe in our study (Figure S7A).

Fjallsjökull retreated by  $\sim 370 \text{ m}$  over the same period (rate of  $31.11 \text{ m a}^{-1}$ ), whilst its proglacial lake, Fjallsárlón also grew in this time, increasing by  $\sim 47\%$  from 2.55 to 3.74  $\text{km}^2$  (growth rate of  $0.1 \text{ km}^2 \text{ a}^{-1}$ ) (Fig. 4B). In comparison, Kvíárjökull only retreated by  $\sim 76 \text{ m}$  between 2010–2020, equating to a rate of  $7.65 \text{ m a}^{-1}$  (Fig. 4B). This represents the smallest change in frontal position observed in this study, and likely reflects a short-term readvance of the northern part of the terminus that occurred between 2012 and 2018 (average change  $\sim +18 \text{ m}$ ) (Figure S6C). Meanwhile, the area of its proglacial lake Kvíárjökulsón grew by  $\sim 46\%$  between 2010–2012 (from 0.41 to 0.60  $\text{km}^2$ ), remained relatively stable between 2012–2018 (fluctuating  $\sim 0.01 \text{ km}^2 \text{ a}^{-1}$ ) and then underwent a further increase of  $\sim 10\%$  between 2018–2020 (from 0.61 to 0.66  $\text{km}^2$ ). Overall, Kvíárjökulsón grew by  $\sim 60\%$  over the study period, from 0.41 to 0.66  $\text{km}^2$  (growth rate of  $\sim 0.03 \text{ km}^2 \text{ a}^{-1}$ ) (Fig. 4B).



**Fig. 4** Cumulative frontal change versus the change in proglacial lake area for (A) the eastern and Western A arms of Breiðamerkurjökull and (B) Fjallsjökull, Kvíárjökull, Svínafellsjökull and Skaftafellsjökull. Data for the two arms of Breiðamerkurjökull, as well

as Fjallsjökull, is for the period 2008–2020, whereas for Kvíárjökull, Skaftafellsjökull and Svínafellsjökull it is for the period 2010–2020. Note that all lake-terminating glaciers have the same marker style as the lake that they terminate into

Svínafellsjökull, meanwhile, retreated by ~100 m between 2010–2020 (rate of 9.78 m a<sup>-1</sup>) (Fig. 4B), which may reflect a slight and partial readvance of the terminus that occurred between 2016 and 2018 (Figure S6D). Despite

this, its proglacial lake grew relatively rapidly in this time, increasing by 133% from 0.21 to 0.49 km<sup>2</sup> (growth rate of ~0.03 km<sup>2</sup> a<sup>-1</sup>) (Fig. 4B), which is similar to the rate of proglacial lake growth observed at Kvíárjökulslón. In

contrast, Skaftafellsjökull retreated by  $\sim 380$  m over the same period (rate of  $37.88 \text{ m a}^{-1}$ ), whilst the area of its proglacial lake increased by 204%, from  $0.56$  to  $1.71 \text{ km}^2$  (growth rate of  $0.11 \text{ km}^2 \text{ a}^{-1}$ ) (Fig. 4B). This represents both the second largest increase in proglacial lake area, and the second fastest rate of proglacial lake growth observed in this study, after Jökulsárlón (Figure S7E).

### 4.3 Ice Surface Elevation Change

Overall, the ice surface elevation change data from Hugonnet et al. [5] indicates that between 2010–2020, the most negative changes occurred at the margins of the five glaciers whilst slightly positive changes occurred in their upper reaches, although there is distinct variability in the pattern of elevation changes observed across the individual glaciers (Fig. 5).

Significant thinning occurred at the calving terminus of the eastern arm of Breiðamerkurjökull over the study period, with  $12.5\text{--}16.5 \pm 0.14 \text{ m a}^{-1}$  of negative surface elevation change observed, with this region extending  $\sim 2$  km back from the front, as well as along the entire width of the calving front (Fig. 5C). These rates of thinning are greater than the change observed at Western A, as well as the other four study glaciers, over the same period. Changes over the rest of the eastern arm range from  $\sim -8.5 \pm 0.14 \text{ m a}^{-1}$  in the lower reaches ( $\sim 3$  km up-glacier) before decreasing with distance up-glacier, with rates of  $-1.5\text{--}2.0 \pm 0.14 \text{ m a}^{-1}$  observed just below the ice fall ( $\sim 25$  km up-glacier). In contrast, the smallest changes in elevation are observed at the margin of Western A, with  $\sim 6.0 \pm 0.14 \text{ m a}^{-1}$  negative change (over

half that observed at eastern arm), which these values again decreasing up-glacier to the main ice fall where  $\sim 1.5 \pm 0.14 \text{ m a}^{-1}$  of negative change occurred (Fig. 5C). Finally, slightly positive changes of  $\sim 0\text{--}2.0 \pm 0.14 \text{ m a}^{-1}$  are observed over the accumulation area of both arms of the glaciers (Fig. 5A).

At Fjallsjökull, up to  $5.0 \pm 0.24 \text{ m a}^{-1}$  of surface thinning is observed at the margin, with this focused over the southern part of the terminus where it extends  $1.5\text{--}2$  km back from the front (Fig. 5B). Rates of thinning then decrease up-glacier to  $\sim 0.5 \pm 0.24 \text{ m a}^{-1}$  just below the main ice fall. In contrast, at Kvíárjökull, the most negative changes in elevation are found just below the main ice fall ( $1.8\text{--}2.8 \pm 0.28 \text{ m a}^{-1}$ ) with these then decreasing slightly up to the margin where between  $+0.5$  and  $-1.5 \pm 0.28 \text{ m a}^{-1}$  of both positive and negative surface changes are observed, respectively (Fig. 5B). In addition, elevation changes over the accumulation area range from between  $+1.3$  to  $-1.5 \pm 0.24 \text{ m a}^{-1}$  at Fjallsjökull and  $+1.0$  to  $-2.5 \pm 0.28 \text{ m a}^{-1}$  at Kvíárjökull (Fig. 5B).

At Svínafellsjökull, whilst rates of thinning in the near-terminus region are relatively small, between  $0.3\text{--}0.8 \pm 0.25 \text{ m a}^{-1}$ , more pronounced negative changes in surface elevation have occurred over the main trunk of the glacier ( $0.5\text{--}6$  km back from the front), where rates of between  $1.0\text{--}2.5 \pm 0.25 \text{ m a}^{-1}$  are observed (Fig. 5A). These then decrease up to below the main ice fall. In comparison, thinning rates of  $6.2\text{--}7.6 \pm 0.17 \text{ m a}^{-1}$  are observed at the margin of Skaftafellsjökull over the same period, with this region of negative elevation changes extending up to  $1.5$  km back from the terminus (Fig. 5A). These then decrease up-glacier to  $\sim 0.5 \pm 0.17 \text{ m a}^{-1}$  just below the main ice fall,

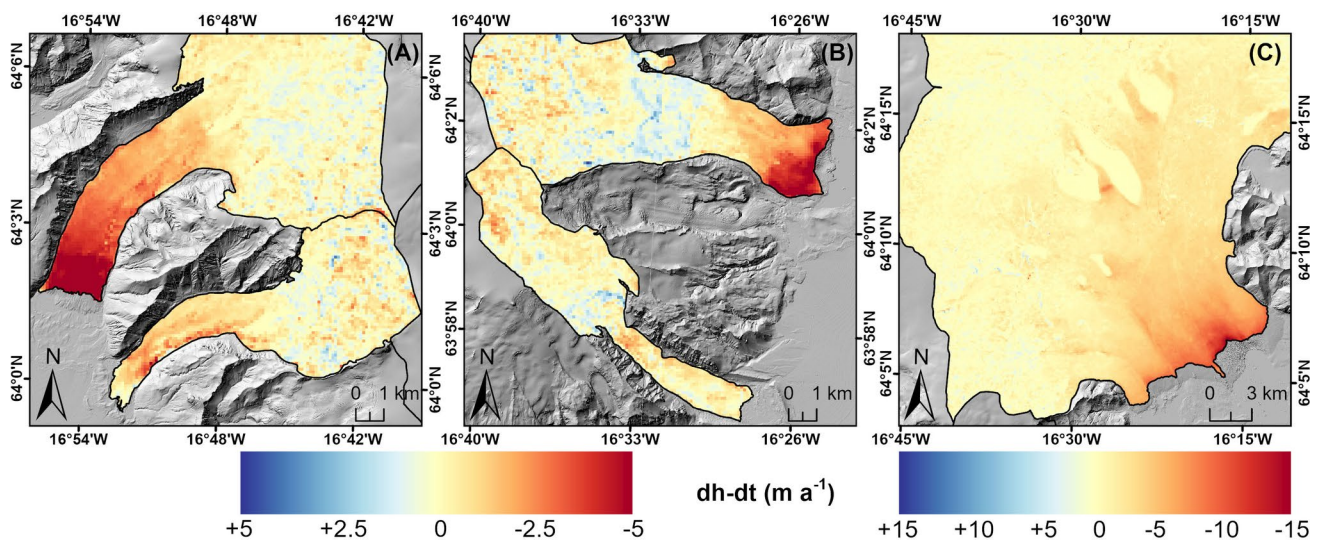


**Fig. 5** Change in ice surface elevation at (A) Skaftafellsjökull & Svínafellsjökull, (B) Fjallsjökull & Kvíárjökull and (C) Breiðamerkurjökull for the period 2010–2020. Panels (A) and (B) share the same legend. Data is from the global ice surface eleva-

tion change dataset by Hugonnet et al. [5]. 2020 glacier outlines are shown in black. Background in each panel is a hillshade of the LiDAR DEM of Iceland from 2016

similar to the pattern observed at Fjallsjökull. Finally, both positive and negative surface changes of between  $+2.5$  to  $-1.5 \pm 0.25 \text{ m a}^{-1}$ , respectively, are observed over the upper reaches of Svínafellsjökull, whilst slightly positive changes of  $0.5\text{--}1.2 \pm 0.17 \text{ m a}^{-1}$  are observed across the accumulation area of the Skaftafellsjökull (Fig. 5A).

## 5 Discussion

We have presented new, detailed insights into the dynamic changes underway at five lake-terminating glaciers in south Vatnajökull for the period 2008/2010–2020. For all glaciers, our data illustrate an overall pattern of increasing velocities over the study period, as well as frontal retreat, proglacial lake growth, and surface thinning, but there is distinct variability in both the patterns and rate of change observed at each individual glacier in each year. In this section, we first compare our velocity, frontal position, and lake area change data to several previous datasets to assess the validity of our findings. We then investigate the dynamic response observed at each glacier and provide a detailed evaluation of the key forcing mechanisms before suggesting what the future response of these glaciers may be. Finally, we discuss the wider implications of our findings in regard to the other lake-terminating outlets of south Vatnajökull.

### 5.1 Comparison to Previous Data

#### 5.1.1 Glacier Velocity

We compare our TerraSAR-X velocities with the ENVEO Icelandic velocity dataset, which was derived through offset tracking of Sentinel-1 SAR images [46], and with the NASA MEaSUREs ITS\_LIVE project, which provides continuous, near-global ice velocities generated using both optical (e.g., Landsat, Sentinel-2) and radar (e.g., Sentinel-1) imagery [47] (Figure S8, S9). To both datasets, we apply the same method that was implemented in this study (detailed in Sect. 3.1.), but due to data availability we only compare velocities from 2016, 2018 and 2020. Overall, there is good agreement between the three datasets, particularly in terms of the spatial velocity patterns observed at each individual glacier, and how these evolve through time. However, there are some differences, for example over faster moving areas of ice (e.g., at the main ice falls), velocities are consistently higher in our data than in either of the other two datasets. In contrast, over slower moving areas of ice, there are a larger number of erroneous points and outliers in the other two datasets (but particularly ITS\_LIVE) than observed in our data.

This is for two reasons: Firstly, where there are sharp velocity gradients present, such as over the ice falls of

both Fjallsjökull and Kvíárjökull, or near the terminus of the eastern arm of Breiðamerkurjökull, the higher resolution of the TerraSAR-X imagery ( $\sim 2 \text{ m}$ ) means such rapid changes in velocity can be more accurately tracked and reproduced (e.g., Figure S8A, S8C, S9A) [38, 48]. In contrast, the coarser resolution of the ENVEO (100 m) and ITS\_LIVE ( $\sim 250 \text{ m}$ ) data means the magnitude of these velocity gradients will have been smoothed over [49, 50]. Similarly, this higher resolution imagery is better able to track and reproduce velocities over slower moving areas of ice, such as accumulation areas, as well as on narrower parts of the main trunks of smaller glaciers (e.g., Kvíárjökull and Svínafellsjökull) than is possible in the other two datasets [38, 51]. Indeed, these regions are less accurately reproduced in the coarser resolution ENVEO and ITS\_LIVE data, resulting in a larger number of erroneous data points and outliers (e.g., over the accumulation areas of both Svínafellsjökull and Skaftafellsjökull, Figure S9B, S9C) [46, 52]. Secondly, our velocity data is generated from imagery acquired predominately in late summer (August–September) with a temporal separation of between 11–33 days (depending on image availability), whereas both the ENVEO and ITS\_LIVE data are annually averaged velocity composites. As such, any particularly large velocity gradients will have been averaged out over the longer temporal baseline of both datasets [38, 53]. Yet despite this, our data still shows good agreement with both these datasets. Furthermore, our data also show good agreement with the few previous studies that have investigated the recent velocity change at several south Vatnajökull glaciers, including Breiðamerkurjökull [30], Fjallsjökull [24] and Kvíárjökull [11], providing further confidence in the validity of our findings.

#### 5.1.2 Frontal Position and Lake Area Change

Our calculated rates of frontal position change show strong agreement with the values reported by Baurley et al. [30] for Breiðamerkurjökull and Dell et al. [24] for Fjallsjökull, as well as by Guðmundsson et al. [22] for all south Vatnajökull glaciers (including Kvíárjökull, Svínafellsjökull and Skaftafellsjökull) over a similar period.

We then compare our digitised proglacial lake areas (and calculated rates of proglacial lake growth) to those of Guðmundsson et al. [22] for the year 2018 (Table S6). Again, we find very good agreement between the two sets of data, particularly when comparing the digitised lake areas from both studies. There is slightly more variation in the calculated rates of proglacial lake growth recorded by both studies (our growth rates are higher in general), but this is because our growth rates are calculated over a shorter period (8–10 years) than those of Guðmundsson et al. [22] (16–27 years). Yet despite these differences in time period, both sets of growth rates still show good agreement. Furthermore, (and

as above) our data also show very good agreement with those studies which have also investigated proglacial lake change at individual south Vatnajökull glaciers, including Briðamerkurjökull [30], Fjallsjökull [24] and Kvíárjökull [11], again providing further confidence in our findings.

## 5.2 Glacier Response 2008/2010–2020 and Future Outlook

### 5.2.1 Briðamerkurjökull

It was suggested by Baurley et al. [30] that the recent retreat and subsequent increase in velocity observed at the eastern arm of Briðamerkurjökull is directly related to the rapid growth of Jökulsárlón (particularly in depth) as the glacier retreated down a reverse bed-slope into the 100–300 m deep bedrock trough it formed during the LIA. This led the authors to propose that velocities may have reached their maximum towards the middle of the last decade in response to this significant deepening of the lake. However, the data from this study importantly indicate that such a dynamic response is ongoing, with velocities and terminus retreat both continuing to increase over recent years (Fig. 2A, 4A, S5C). For example, mean near-terminus velocities in 2015 were  $1.64 \text{ m d}^{-1}$  [30], whereas in 2020 they were  $\sim 2.45 \text{ m d}^{-1}$  (this study,  $\sim 50\%$  increase). Similarly, the eastern arm retreated by  $\sim 400 \text{ m}$  between 2014–2018 [30], yet between 2018–2020 it receded by  $\sim 250 \text{ m}$  (this study), which is over half the retreat observed in 2014–2018.

Based on these observations, it is likely that initial retreat into deeper water resulted in an increase in buoyant forces acting on the terminus, reducing the effective pressure (and consequently the basal drag), leading to an increase in velocity [54–57]. This, in turn, will have caused the glacier to extend and thin, steepening the ice surface and causing a further increase in velocity by increasing the driving stress [19, 58, 59]. This will have resulted in increased fracture propagation at the terminus, leading to an increase in calving activity and subsequently, the rate of retreat [20, 24, 60].

Continued retreat into deeper water will have triggered a further increase in buoyant forces, causing an additional increase in velocity, thinning, calving, and retreat (as observed in our data) and resulting in the implementation of a positive feedback mechanism termed “dynamic thinning” (e.g., [55, 57, 61, 62]) that is driving the current unstable dynamic behaviour of the glacier [30]. This may explain why the near-terminus region of the eastern arm thinned by  $\sim 100\text{--}150 \text{ m}$  between 2010–2020 (Fig. 5C) which is significantly greater than the rate of change observed at the calving front of the other glaciers in this study. This response may be exacerbated by the fact that ice flow from the interior cannot balance the substantial losses occurring at the terminus, further increasing the ice

velocity and rate of retreat [30, 63] and providing clear evidence that the dynamic behaviour of the eastern arm has become decoupled from local climate.

In addition, such a dynamic response is likely to continue in future as the eastern arm continues to retreat through its deep bedrock trough [29], which radio-echo sounding surveys undertaken in the 1990s revealed was  $\sim 20 \text{ km}$  long [35]. As of 2020, this bedrock trough still extends some  $\sim 12 \text{ km}$  back from the terminus, with the first  $\sim 2 \text{ km}$  characterised by a depth of  $\sim 200 \text{ m}$  and the remaining  $\sim 10 \text{ km}$  characterised by a depth of  $\sim 100\text{--}150 \text{ m}$  (Fig. 6). Therefore, and assuming a similar retreat rate as observed in this study, over the next 10 years, the eastern arm will still be retreating through one of the deepest parts of its trough (Fig. 6) and as such the dynamic processes observed here will continue to drive the dynamics and retreat patterns of this arm of Briðamerkurjökull. This unstable dynamic behaviour will continue until it begins to retreat out of the deep bedrock trough into shallower water, which modelling studies suggest will not be until at least  $\sim 2100$  (e.g., [64, 65]), at which point it may then begin to stabilise.

In contrast, the recent changes at Western A are more muted, with significantly slower velocities, less retreat and little change in proglacial lake area observed over our study period (Fig. 2B, 4A), which agree with the finding of Baurley et al. [30]. This likely reflects the specific bed topography of Breiðárlón, which is much shallower than Jökulsárlón ( $< 40 \text{ m}$  deep in 2018), as well as its ongoing sedimentation, which has caused it to remain stable over recent years [22]. However, velocities over this arm of the glacier did increase steadily over our study period, particularly in the near-terminus region (333% increase, Fig. 2B), suggesting that over recent years the influence of Breiðárlón on the near-terminus dynamics of Western A may have also increased (e.g., through calving).

Importantly, this influence may become more pronounced in future as this arm of the glacier continues its retreat through its  $\sim 9 \text{ km}$  long, max.  $\sim 30 \text{ m}$  deep bedrock trough [35]. Indeed, while the 2020 terminus is located in relatively shallow water ( $\sim 9 \text{ m}$  deep),  $\sim 1 \text{ km}$  back from this location the bed slope continues to reverse into deeper water ( $\sim 30 \text{ m}$  deep), resulting in a long and narrow bedrock trough that extends  $\sim 4 \text{ km}$  into the interior of the glacier (Fig. 6). Therefore, although in 10 years' time the glacier terminus will still likely be grounded in relatively shallow water (assuming a similar rate of retreat as observed in this study), there is the possibility that in future the influence of Breiðárlón may develop to such an extent that it can begin to impact the dynamics and retreat patterns of this arm of the glacier, similar to what is currently underway at the eastern arm, but at a much smaller scale and magnitude.

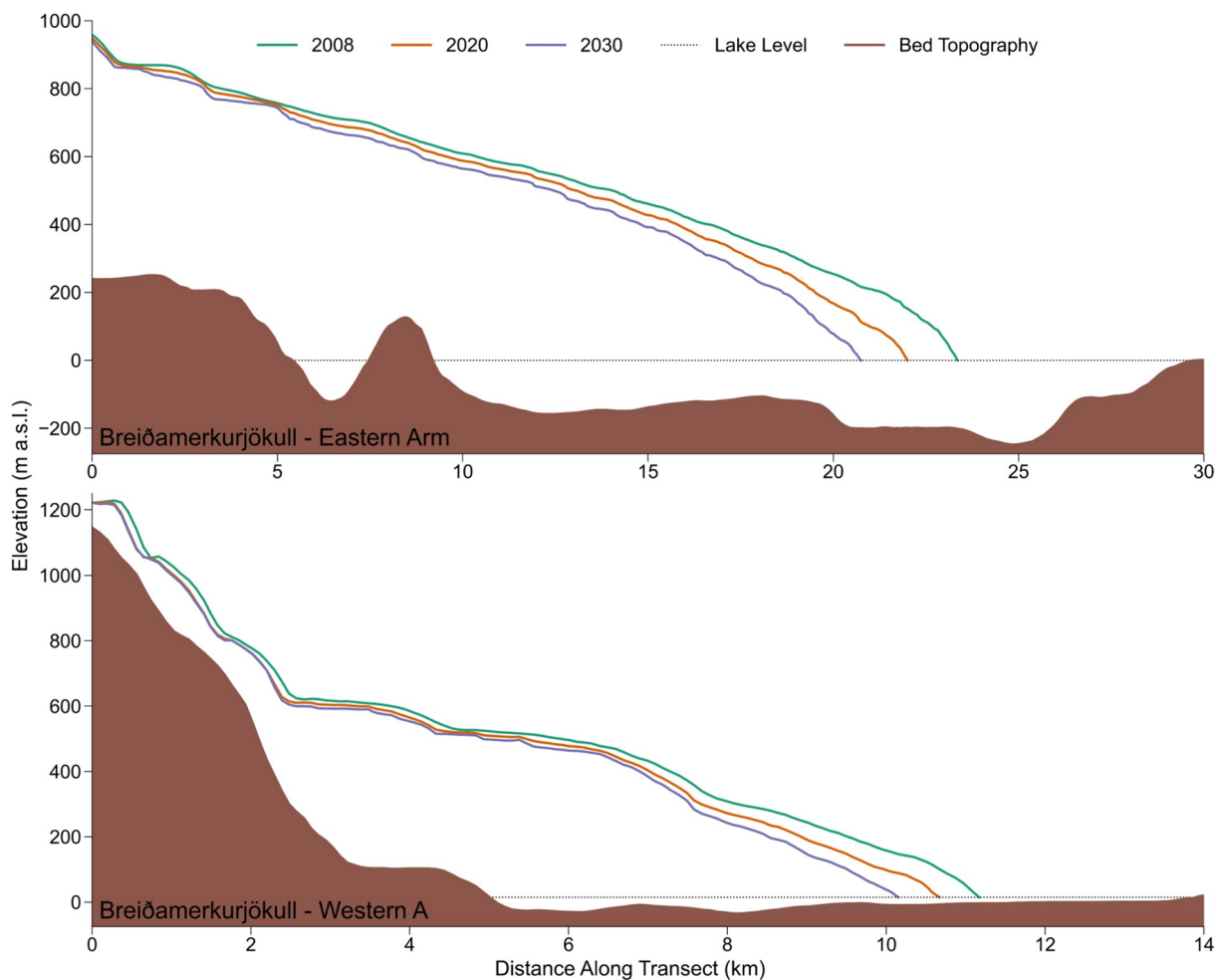


**Fig. 6** Longitudinal profiles for the eastern and Western A arms of Breiðamerkurjökull, illustrating the position of the terminus and ice thickness in 2008, 2020 and 2030. Surface profiles were calculated using data from this study, the LiDAR DEM of Iceland, and the surface elevation change dataset of Hugonnet et al. [5]. Bed profiles were

extracted from the Breiðamerkurjökull bedrock topography dataset illustrated in Fig. 1. Dotted lines indicate proglacial lake level in 2020. Further detail on how individual profiles were derived can be found in Table S7

### 5.2.2 Fjallsjökull

A similar dynamic response to that observed by Baurley et al. [30] at the eastern arm of Breiðamerkurjökull has also been observed at the neighbouring glacier Fjallsjökull by Dell et al. [24]. Indeed, the authors suggest that the increased velocities and heightened retreat rate observed since the early 2000s directly corresponds to the rapid expansion of Fjallsárlón and subsequent retreat of the glacier back into its ~200 m deep bedrock trough, resulting in an increase in buoyant forces and the implementation of the same positive feedback mechanism described previously. Furthermore, the data from this study also suggest that such a dynamic response is ongoing, just like at the eastern arm of Breiðamerkurjökull.

Indeed, we observe an almost 500% increase in mean near-terminus velocities since 2008, which peak

at  $\sim 0.82 \pm 0.09 \text{ m d}^{-1}$  in 2020 (Fig. 2C). This is a similar magnitude to, but noticeably larger than, the  $\sim 0.5 \text{ m d}^{-1}$  observed by Dell et al. [24] over the same region in 2017/2018. Our data also seem to indicate that from 2018 onwards, velocities in the near-terminus region (within ~2 km of the front) begin to increase up to the calving front, rather than decrease (Fig. 2C). This is similar to the pattern observed at the eastern arm of Breiðamerkurjökull over the study period and may reflect the ongoing dynamic evolution of the glacier as it continues its retreat through its deep bedrock trough. We also observe a further increase in the both the size of Fjallsárlón and the cumulative retreat of the glacier since 2016 (Fig. 4B, the last year that Dell et al. [24] obtained this data), providing further support to the assertion that the dynamic response originally observed by the authors is ongoing.

In addition, the data from this study also seem to indicate that there is a non-uniform pattern of negative surface elevation changes near the terminus of Fjallsjökull (Fig. 5B). Indeed, the most negative elevation changes are found over both the central, and in particular, the southern part of the terminus ( $\sim 5.5 \pm 0.24 \text{ m a}^{-1}$ ), encompassing a  $\sim 2 \text{ km} \times \sim 2 \text{ km}$  region, whereas significantly smaller elevation changes (in both magnitude and extent) are observed over the northern part of the terminus ( $\sim 2.8 \pm 0.24 \text{ m a}^{-1}$ ). This contrasts with the more homogenous pattern of negative surface elevation changes observed near the terminus of the eastern arm of Breiðamerkurjökull. Such a pattern is likely the result of a deeply incised bedrock channel that sits within the main  $\sim 3 \text{ km} \times 4 \text{ km}$  bedrock trough found under the glacier [23]. Importantly, this deep bedrock channel, which is  $\sim 2 \text{ km}$  by  $\sim 2 \text{ km}$  and  $\sim 120 \text{ m}$  deep at its maximum, directly underlies the southern part of the present-day terminus [24, 31]. As such, the terminus is currently retreating through the deepest part of the channel in this region, meaning velocities, and consequently the rate of surface thinning, will be elevated (Fig. 7) (e.g., [59, 62]). Indeed, the location of this channel coincides with the region of the terminus where velocities are at their highest, suggesting that dynamic thinning may have recently been initiated in this region of Fjallsjökull [24, 31], and that the dynamic behaviour of this region of the glacier may have also become decoupled from the local climate as a result.

Furthermore, such a dynamic response will continue in future as this part of the glacier continues its retreat through the southern bedrock channel. As of 2020, the channel still extends  $\sim 1 \text{ km}$  back from the terminus, with much of this characterised by a depth of  $\sim 80\text{--}100 \text{ m}$  (Fig. 7). The main bedrock trough under Fjallsjökull then extends for another  $\sim 1.5 \text{ km}$  after this, but at a much shallower depth ( $< 50 \text{ m}$ ) (Fig. 7). Therefore, and assuming a similar retreat rate as observed in this study, over the next 10 years this region of Fjallsjökull will still be retreating through one of the deepest parts of the southern bedrock channel (Fig. 7), meaning the dynamic processes observed here will continue to drive the dynamics and retreat patterns of this region of glacier until it retreats into shallower water.

A similar response may also be observed at the main flowline (centreline) of the glacier, which is currently retreating through the main bedrock trough. As this trough still extends for another  $\sim 2.5 \text{ km}$  back from the terminus, with the majority of this characterised by a depth of  $\sim 50\text{--}80 \text{ m}$ , it is likely that in 10 years' time this region of the glacier will also still be retreating through one of the deepest parts of its main bedrock trough (Fig. 7), with similar consequences for the dynamics of this region of the glacier. Finally, while another, deeper, bedrock channel is found under the northern part of the terminus ( $\sim 200 \text{ m}$  deep), the glacier front in this region is presently grounded in very shallow water (Fig. 7).

This may explain why relatively slow velocities (Figure S3) and less-negative elevation changes (Fig. 5B) are currently observed in this region. Although this is unlikely to change significantly in the near future (i.e., 10 years' time, Fig. 7), once the terminus does begin to retreat into deeper water then it is likely that the dynamic behaviour will evolve in a similar way to what is presently observed over the southern bedrock channel, with elevated velocities, frontal retreat, and thinning rates occurring as a result.

### 5.2.3 Kvíárjökull

In contrast to both Fjallsjökull and the eastern arm of Breiðamerkurjökull, the dynamics of Kvíárjökull are unlikely to have been driven by proglacial lake expansion and the retreat of the glacier into deeper water. Indeed, the area of Kvíárjökull only increased by  $\sim 0.25 \text{ km}^2$  over the study period, whilst the terminus receded by only  $\sim 76 \text{ m}$  (Fig. 4B), which represents both the smallest increase in proglacial lake area and change in front position observed in this study. Furthermore, the terminus is presently situated at the outer edge of its proglacial lake, which when combined with the small variations in lake growth and frontal position, suggest that other factors are driving the dynamic behaviour of this glacier.

Previous research has demonstrated that the dynamics of Kvíárjökull are primarily controlled by a narrow flow corridor located along its central axis, which is surrounded by slower moving or stationary lateral and latero-terminal regions [66, 67]). This active flow corridor does not move as one complete unit, rather it comprises several individual lobes that move independently (or 'pulse') in surge-like movements down-glacier, with flow directed towards the northeastern part of the margin [11, 67]. Therefore, the glacier is characterised by periods (or 'pulses') of increased ice flow separated by periods of 'quiescence', with the pulse-like activity occurring over decadal time-scales [67].

Based on the data from this study, the most recent period of increased ice flow likely occurred at some point between 2012 and 2016. This is evidenced by mean-terminus velocities peaking at  $\sim 0.42 \pm 0.09 \text{ m d}^{-1}$  in 2016 (increasing from  $\sim 0.19 \pm 0.09 \text{ m d}^{-1}$  in 2012, Fig. 3A, S3), and by a clear re-advance of the northeastern part of the margin over the same period which narrowed the connection between the northern and southern parts of Kvíárjökull (Figure S6C). Mean-terminus velocities then begin to decrease, marking the end of the speed-up event, however, the northeastern part of the margin remains relatively stable up until 2020, despite the presence of Kvíárjökull at its northern and southern boundary. This is likely a result of the continual movement of mass down-glacier by the active flow corridor (e.g., [66, 67]), as well

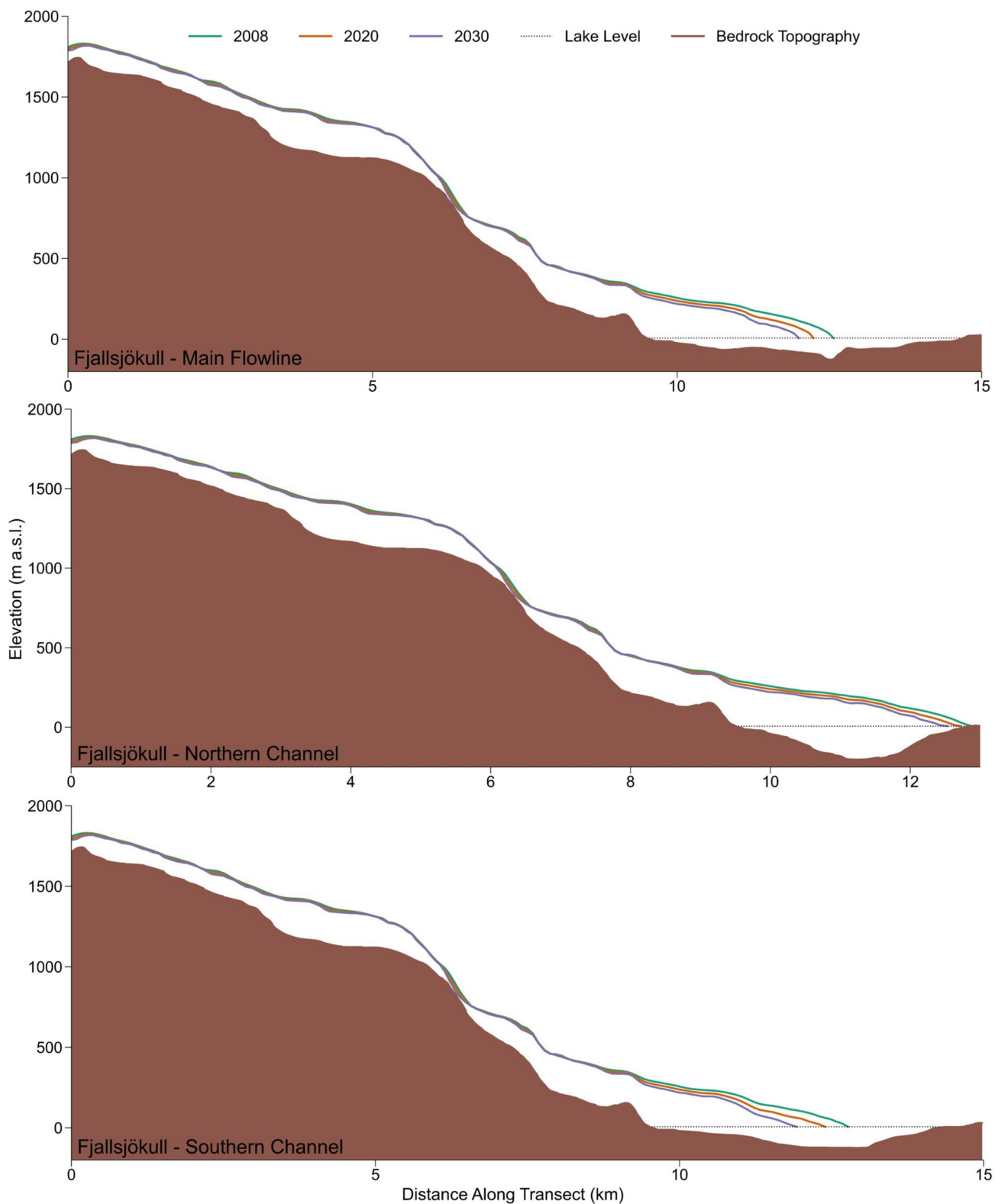


**Fig. 7** Longitudinal profiles for the main flowline, northern channel, and southern channel regions of Fjallsjökull, illustrating the position of the terminus and ice thickness in 2008, 2020 and 2030. Surface profiles were calculated using data from this study, the LiDAR DEM of Iceland, and the surface elevation change dataset of Hugonnet

et al. [5]. Bed profiles were extracted from the Fjallsjökull bedrock topography dataset illustrated in Fig. 1. Dotted lines indicate proglacial lake level in 2020. Further detail on how individual profiles were derived can be found in Table S7

as the insulating effect of the thick layer of supraglacial debris cover in this region (e.g., [68, 69]), which may also explain why the most negative elevation changes are found below the main ice fall, not at the terminus as has been observed at other glaciers in this study (Fig. 5B).

In comparison, the southeastern part of the margin is far more sensitive to the presence of Kvíárjökulslón, which is primarily due to the relatively flat and thin nature of the ice surface [11, 67]. This means that the lake can often inundate the glacier front, causing it to destabilise and possibly disintegrate due to the processes of frontal ablation and related thermo-mechanical processes (e.g., [70]). This may explain why the area of Kvíárjökulslón grew so rapidly between 2010–2012 (from 0.41 to 0.60 km<sup>2</sup>, Fig. 4B, S7C) and why the southeastern part of the margin also retreated significantly over the same period (Figure S6C). In contrast, the readvance of the northeastern part of the margin between 2012–2016 may have caused the southeastern part to temporarily stabilise, and, as was observed in 2018, even undergo a slight readvance (Figure S6C), which was primarily driven by an overriding flow unit (or ‘lobe’) immediately up-glacier [67]. Such a response may explain why the area of Kvíárjökulslón, as well as the position of the terminus in this region, remained relatively stable during this time (Fig. 4B, S6C, S7C). However, between 2018–2020 the terminus in this region retreated relatively rapidly (~100–150 m), resulting in a relatively large increase in the area of Kvíárjökulslón (Fig. 4B), and indicating that this region is again being impacted by the processes of frontal ablation and the related thermo-mechanic properties of the lake (e.g., [11]).

Like many of the other southern outlets of Vatnajökull, Kvíárjökull is also underlain by a relatively large bedrock trough, which extends ~4 km back from the present-day terminus and has a maximum depth of ~100 m [23]. Yet despite the 2020 terminus being located above the deep reverse-sloping part of the trough (Fig. 8), it is unlikely that the glacier will undergo a similar dynamic response to what is currently underway at Fjallsjökull and the eastern arm of Breiðamerkurjökull. This is because the southeastern part of the terminus (where the deepest parts of the trough are located) is likely to be floating, meaning it is not physically grounded in, or retreating into, deeper water. Indeed, field observations indicate that the terminus is relatively flat and thin in this region (and therefore stagnant), which allows lake water to propagate under and up into the glacier, inundating the ice surface and resulting in the calving of large tabular blocks (e.g., [11]).

Although it is unclear when the switch from a grounded to a floating ice front occurred, it was likely driven by a change in ice thickness relative to water depth (i.e., thinning), and a subsequent increase in buoyant forces, resulting in uplift of the glacier terminus (e.g., [56, 71]). As such, over the next 10 years the southeastern part of the margin will

continue to retreat rapidly in response to the inundation and destabilisation by Kvíárjökulslón (Fig. 8), as has recently been observed by Kavan et al. [11]. This may have significant implications for the overall stability of the floating portion of the glacier margin, which may undergo complete terminus break-up and disintegration in future. In contrast, the northeastern part of the margin will likely remain stable for the foreseeable future due to the continual inflow of mass into the region, as well as its thick layer of supraglacial debris cover (e.g., [67, 68]).

#### 5.2.4 Svínafellsjökull

Of the five glaciers investigated in this study, it is the dynamics of Svínafellsjökull that have undergone the least change over our study period, and in fact have remained relatively stable. Indeed, our data indicate a gradual increase in mean near-terminus velocities, a relatively modest rate of surface thinning, and only ~97 m of terminal recession in this time. Although proglacial lake expansion (and related dynamic effects) can explain some of the observed dynamic variations, it is likely that several other factors may also be exerting a key control.

With a mean slope of ~9.0°, Svínafellsjökull is the one of the steepest outlets of Öraefajökull [25], and the steepest outlet investigated in this study. Yet despite this, the lower ~6 km of the glacier is characterised by a relatively gentle surface slope (~3°) (Fig. 8), which would result in a down-glacier reduction in driving stress. This, combined with the narrow valley in which the glacier is situated (which increases the lateral resistive stresses), may explain why we observe relatively low velocities in the lower part of the glacier [19, 72, 73]. However, this reduction in driving stress does not explain why we observe a gradual increase in near-terminus velocities over our study period, from ~0.12 to ~0.19 ± 0.09 m d<sup>-1</sup> (58% increase, Fig. 3B). Instead, this gradual acceleration is likely a result of the growth and expansion of the two proglacial lakes on the northern and southern side of the terminus (Figure S7D). This would have increased the area of the terminus that is in contact with the lakes, and consequently, the extent to which these lakes could influence near-terminus dynamics, leading to a further reduction in the effective pressure, increased basal sliding and resulting in the observed gradual increase in velocity [20, 54].

In addition, the valley of Svínafellsjökull widens ~2 km up-glacier from the terminus, allowing the glacier to spread and resulting in an extensional flow regime (e.g., [74]) (Figure S6D). Importantly, this extensional regime may influence near-terminus dynamics through increased surface thinning, which when combined with surface melt may have caused the southern part of the terminus to be subjected to increased buoyant forces, which continued to evolve until

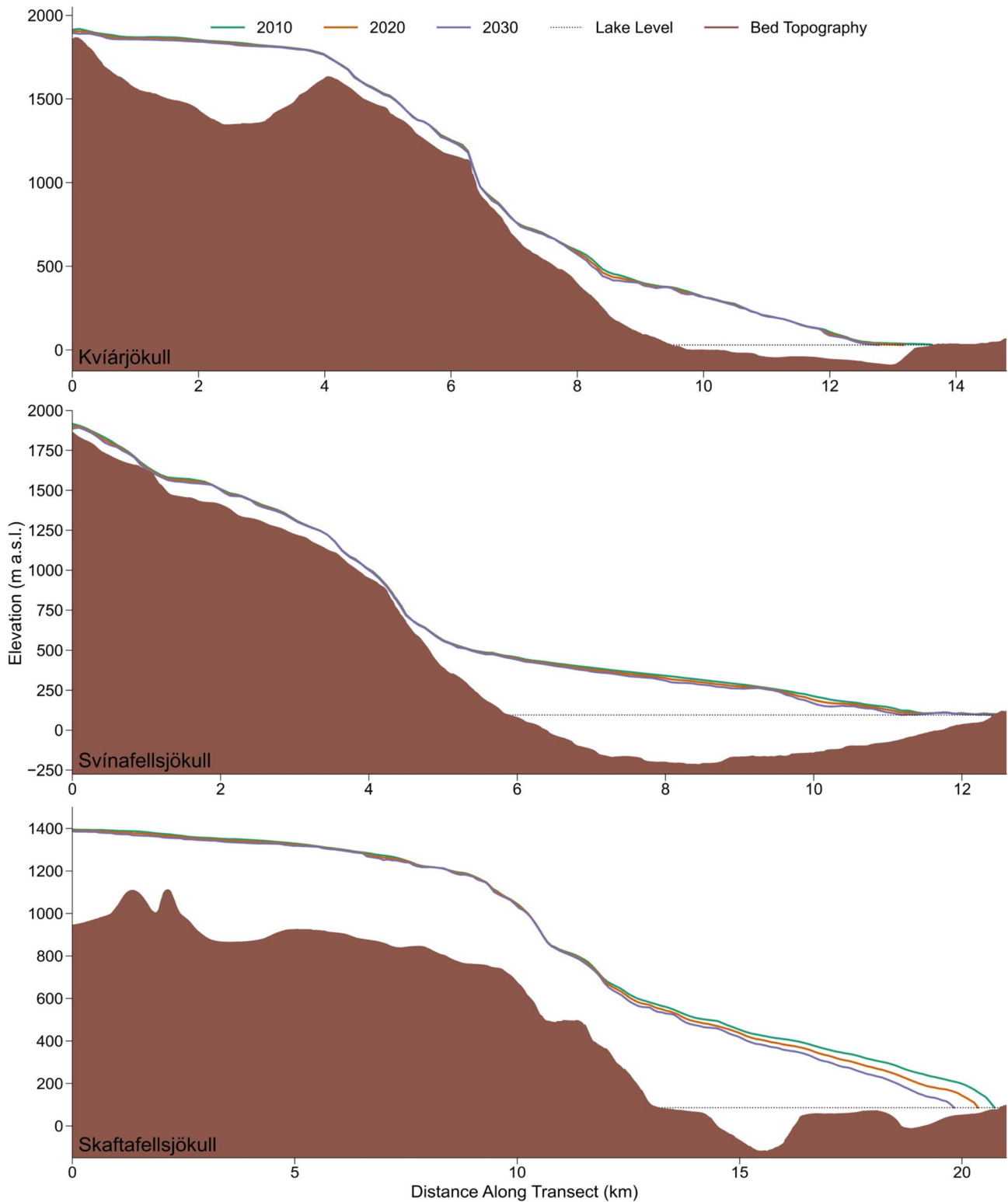


**Fig. 8** Longitudinal profiles for Kvíárjökull, Svínafellsjökull and Skaftafellsjökull, illustrating the position of the terminus and ice thickness in 2010, 2020 and 2030. Surface profiles were calculated using data from this study, the LiDAR DEM of Iceland, and the surface elevation change dataset of Hugonnet et al. [5]. Bed profiles for

each glacier were extracted from the relevant bedrock topography dataset illustrated in Fig. 1. Dotted lines indicate proglacial lake level in Fig. 1. Further detail on how individual profiles were derived can be found in Table S7

partial floatation occurred (e.g., [55, 71]). Surface thinning will also result in a reduction in the effective pressure, meaning it is possible that this thinning may have also contributed to the observed gradual increase in near-terminus velocities (e.g., [54, 57]). Although terminus floatation can result in rapid ice marginal retreat and terminus disintegration via calving (e.g., [71, 75, 76]), the reason this has yet to occur at the southern margin of Svínafellsjökull is because parts of the terminus are grounded on bedrock at the outer extent of the lake, despite the terminus itself being relatively flat and thin (Fig. 8). This, combined with the continual inflow of mass to the region (due to the gradual increase in velocities), means the high stresses present at the margin can be accommodated, allowing the terminus to remain relatively stable (e.g., [71]). This continued inflow of mass to the terminus may also explain the relatively low rates of thinning observed in this region (Fig. 5A).

Furthermore, parts of the both the central and northern terminus are also grounded on bedrock at the outer extent of the lake (Figure S6D) and as such these regions have also remained stable, which may help to explain why the margin of Svínafellsjökull only retreated by ~97 m over our study period. Whilst the rate of retreat was consistent over the study period (Fig. 4B), it was not homogenous across the entire terminus, with much of the recession focused over the lateral margins of the northern and southern parts of the terminus where it terminates in a lake but is not grounded on bedrock (Figure S6D). In these regions the influence of the thermo-mechanical properties of the lake are greatest, and as such it is likely that calving is actively occurring, either through thermal melt and notch formation, or through buoyant forces acting on the terminus and the propagation of basal crevasses (e.g., [31, 59, 75, 77]). Therefore, whilst the overall pattern is one of terminus retreat, the relatively stable nature of large parts of the terminus means the retreat rate is low.

An additional factor which may have influenced the observed dynamic variations is the occurrence of a large landslide in 2013, which caused a ~1.7 km<sup>2</sup> area of the ice surface to be covered in a thick layer of debris (Fig. 2 in [78]). While the ice underneath the debris has been efficiently insulated and protected from surface melt, the ice immediately surrounding it has seen enhanced melt due to the fine layer of dust that settled on the surface post-landslide (e.g., [68, 69, 79]). This resulted in a 35 m difference in surface elevation between the two regions by 2020 [78]. Although the impact of the landslide is not present in our surface elevation data (which cover the period 2010–2019), it's probable that its occurrence will have contributed to several of the other dynamic variations observed in this study. For example, the difference in elevation between the debris covered- and clean-ice areas will have increased the surface slope, causing an increase in the driving stress and

thus velocities, which in turn will have provided additional resistive stresses to the partially floating southern terminus, helping it to remain stable. In addition, this landslide material is continually being advected down-glacier (it was advected ~1 km between 2013–2020), and as such these processes are likely to continue in future as it is transported towards the southern margin, where it will likely lead to further stabilisation, incremental stagnation, and the potential formation of a dead-ice environment [78].

Based on the data presented in this study, it is unlikely that the dynamics of Svínafellsjökull will significantly change or evolve over the coming decade, despite the presence of a 300 m deep bedrock trough under the glacier, which extends ~6 km back from the present-day terminus [22, 23]. This is because rapid retreat and terminus disintegration is unlikely whilst much of the margin remains grounded on stable bedrock at the lake edge, a factor that will be further influenced by the continued down-glacier advection of the landslide material, which as mentioned previously may further stabilise the southern margin through the formation of a dead-ice environment. As such, by 2030 this part of the margin is still likely to be grounded at the lake edge (Fig. 8).

In contrast, it is more likely that the northern part of the terminus will undergo rapid retreat in future, as although the terminus is grounded (i.e., not floating), it is beginning to detach from the surrounding bedrock, while at the same time its proglacial lake is growing relatively rapidly (Figure S6D, S7D). This indicates an increasing influence of the lake and calving on terminus stability, and as such in the near future this part of the glacier may begin retreating down its reverse bed slope into deeper water, leading to increased velocities, thinning, and thus further calving and retreat (e.g., [30, 58, 80]). Indeed, it is likely that calving will play an important role at both proglacial lakes in future as they continue to grow, resulting in continued terminus retreat and the potential detachment of large parts of the terminus from its surrounding bedrock, with implications for the stability of the lower part of the glacier.

### 5.2.5 Skaftafellsjökull

In contrast to Svínafellsjökull, the dynamic behaviour of Skaftafellsjökull has evolved considerably over the study period, with the second largest change in front position (~380 m), second highest rate of terminus thinning ( $\sim 7.6 \pm 0.17 \text{ m a}^{-1}$ ), and third highest growth in proglacial lake area (~1.1 km<sup>2</sup>) observed at this glacier. Surface velocities also increase significantly over the study period, particularly near the terminus (Figure S5A), suggesting that the dynamics of the glacier are likely being influenced by

the growth of the proglacial lake and retreat of the terminus into deeper water.

In 2010, the terminus of Skaftafellsjökull was grounded in shallow water (~ 12 m deep) on a relatively flat region of bedrock near the edge of the lake (Fig. 8). As such the influence of the lake on the dynamics of the glacier were limited, which may explain why near-terminus velocities were low in 2010 and remained as such in 2012 ( $\sim 0.05 \pm 0.09 \text{ m d}^{-1}$ ). Instead, it is likely that during this time the dynamics of the glacier were primarily controlled by air temperatures (e.g., [25]). Yet while this would have resulted in the observed terminus recession of ~ 95 m between 2010–2012 (Fig. 4B), as well as some of the observed surface thinning (via surface melt), overall, the glacier was relatively stable during this time (Figure S6E). However, at some point between 2012 and 2016, the continued retreat of the glacier caused the grounded terminus to recede past the flat region of bedrock and begin retreating down a much steeper, reverse bed slope into deeper water (Fig. 8).

This would have increased the buoyant forces acting on the terminus, reducing the effective pressure and causing velocities to increase [54, 55]. Increased velocities will, in turn, have caused the ice surface to extend and thin, leading to increased calving, terminus retreat, and a further increase in velocities [19, 58, 59]. Such a response can be observed in our data, with mean near-terminus velocities increasing by ~ 160% from ~ 0.05 to  $0.13 \pm 0.09 \text{ m d}^{-1}$  (Fig. 3C), and a steady increase in both the rate of terminus retreat and proglacial lake growth over the same period (Fig. 4B). Importantly, our data indicate that this dynamic response has continued, at least until the end of the study period, with a further increase in velocities, terminus retreat and lake growth observed between 2016–2020 (Fig. 3C, 4B, S6E, S7E), strongly suggesting that the same positive feedback mechanism already underway at both Fjallsjökull and the eastern arm of Breiðamerkurjökull may have recently been initiated at Skaftafellsjökull.

This increase in velocity may also explain why we observe such high rates of surface thinning at the terminus of Skaftafellsjökull over the study period (Fig. 5A). Indeed, while some of the observed thinning can be attributed to surface melt (e.g., [14, 25]) the magnitude of this thinning ( $\sim 7.6 \pm 0.17 \text{ m a}^{-1}$ ) can only have occurred in response to ice dynamics, i.e., through dynamic thinning (e.g., [57, 60]). Furthermore, thinning itself also reduces the effective pressure, and therefore it is likely that the high thinning rates will have also contributed to the observed rapid increase in near-terminus velocities (e.g., [54, 57]), providing further evidence that the growth of the proglacial lake and retreat of the glacier into deeper water are now driving the dynamic behaviour of the glacier.

In addition, this dynamic response may have been enhanced between 2018–2020 due to an increase in the

gradient of the reverse bed, which led to a more rapid increase in water depth between the two years (Fig. 8). Indeed, in 2018 the water depth at the terminus was ~ 24 m, whereas in 2020 it was ~ 30 m. Consequently, while terminus water depth increased by ~ 150% between 2010–2020 (12 m to 30 m), one third of this increase occurred between 2018–2020 (i.e., within two years). This would have triggered a rapid increase in buoyant forces, further reducing the effective pressure and resulting in an additional increase in velocities, calving, and retreat [19, 59]. Importantly, the impact of this rapid increase in water depth is clearly observed in our data. For example, near-terminus velocities increased from ~ 0.17 to  $\sim 0.30 \pm 0.09 \text{ m d}^{-1}$  over the two years (~ 76% increase, Fig. 3C), whilst the terminus itself retreated by ~ 120 m over the same period, which means that one third of the total retreat that occurred between 2010–2020 did so between 2018–2020 (Fig. 4B, S6E). Such a dynamic response illustrates how small, but rapid, changes in water depth can have a significant impact on the dynamics of lake-terminating glaciers.

However, in spite of these recent variations, there's the possibility that the dynamics and retreat of Skaftafellsjökull may begin to stabilise towards the end of the decade, despite the presence of the ~ 200 m deep, ~ 6 km long bedrock trough under the glacier (Fig. 8) [22, 23]. This is because immediately up-glacier of the 2020 terminus the gradient of the bedrock slope reduces significantly due to the presence of a ~ 400 m long region of relatively flat bedrock (Fig. 8). Consequently, rapid increases in water depth, as observed between 2018–2020, will not be able to occur. This means that the likelihood of the glacier undergoing rapid changes in ice dynamics may also be reduced. Indeed, based on the retreat rate calculated in this study, by 2030 the terminus of Skaftafellsjökull will most likely be grounded on this region of flat bedrock (Fig. 8) and, therefore, its dynamics may have begun to stabilise.

On the other hand, there is also the possibility that the observed recent rapid retreat may have caused the dynamics of the glacier to become partly decoupled from the local climate, meaning such a dynamic response will be maintained regardless of any future change in the gradient of the bedrock slope. This is supported by our observations from Fjallsjökull and the eastern arm of Breiðamerkurjökull, both of which see a continuous increase in their velocities and terminus retreat over the study period, despite both glaciers having retreated over the deepest parts of their respective bedrock troughs (i.e., the water depth has decreased) (Fig. 6, 7). As such, there is the strong possibility that the dynamics of Skaftafellsjökull will continue to evolve in future as it continues its retreat through its deep bedrock trough, resulting in a heightened dynamic response that is decoupled from climate, similar to that already observed at Fjallsjökull and the eastern arm of Breiðamerkurjökull over recent years.

### 5.3 Implications for the other Outlets of South Vatnajökull

The findings of this study highlight the importance of proglacial lake growth in driving the dynamics and retreat patterns of glaciers in Iceland, with such a pattern likely to continue in future as they further grow and develop. In addition, there is the strong possibility that the other southern outlets of Vatnajökull will also undergo a similar dynamic response in future, particularly those to the east of Breiðamerkurjökull. Indeed, many of these outlets also have reverse-sloping beds that sit some 200–300 m below the current elevation of their termini, including Skálafellsjökull (~ 3 km long, ~ 200 m deep), Heinabergsjökull (~ 11 km long, ~ 200–300 m deep), Fláajökull (~ 5 km long, > 200 m deep) and Hoffellsjökull (~ 7 km long, ~ 250 m deep), and as such they have also seen the rapid growth and expansion of proglacial lakes at their margins in recent years [22, 25]. This has also resulted in accelerated terminus retreat and mass loss via calving, although as was observed in this study, different glaciers often display contrasting dynamic behaviour, highlighting the need for further work in this region.

As a result, in order to better understand the influence of proglacial lake growth on the dynamics of the southern lake-terminating glaciers of Vatnajökull, and to determine whether their contribution to the overall mass loss of the ice cap may increase in future, additional, multi-method and multi-temporal analyses are required, such as those by Dell et al. [24], Baurley et al. [30], and the work presented here. In addition, detailed in-situ field measurements of lake depth, above-waterline ice thickness and ice surface slope in the vicinity of the calving front, as well as observations of specific calving style, are needed to better understand the factors controlling the dynamics of individual glaciers. Such data could then be used to help further constrain calving processes in glacier and ice sheet models, allowing the future patterns of retreat and mass loss, and subsequently the SLR contribution, of these rapidly changing lake-terminating glaciers to be more accurately quantified.

## 6 Conclusions

In this study, we utilised satellite remote sensing to investigate the recent dynamic changes and likely future evolution of five lake-terminating glaciers draining the south Vatnajökull ice cap between 2008/2010–2020. Overall, our data show an increase in velocity at all five glaciers over the study period, as well as widespread frontal retreat, proglacial lake growth and terminus thinning, although the magnitude of these variations differed significantly between individual glaciers. The greatest changes in dynamics were observed at the eastern arm of Breiðamerkurjökull, Fjallsjökull, and

Skaftafellsjökull, and likely occurred in response to proglacial lake growth and the retreat of each glacier down a reverse bed slope into deeper water. This would have increased the buoyant forces acting on the terminus, reducing the effective pressure and triggering an increase in velocities. Increased velocities will, in turn, have caused the ice surface to extend and thin, leading to increased calving, terminus retreat, and resulting in a further increase in velocities (i.e., dynamic thinning). This strongly suggests that the behaviour of each glacier has become decoupled from the local climate, with such a response likely to continue in future.

This is in stark contrast to the dynamic variations observed at Kvíárjökull and Svínafellsjökull over the same period. At Kvíárjökull, due to the pulse-like flow of the glacier, the northeastern part of the margin re-advanced between 2012–2016, and although velocities decreased after 2016, the terminus in this region remained stable until the end of the study period. In contrast, the southeastern part of the margin is afloat in the lake, and while it was stable during the period of readvance, since 2018 it has begun to break up and disintegrate, resulting in rapid retreat. The dynamics of Svínafellsjökull, meanwhile, underwent the least change over the study period because large parts of the terminus are grounded on bedrock at the outer edge of the lake, keeping the glacier relatively stable. However, continuous proglacial lake growth at both the northern and southern margin over recent years have caused parts of the terminus to become afloat, and as such once the glacier begins to detach from the bedrock it will likely undergo rapid and unstable retreat.

The different forcing mechanisms observed in this study may also be analogous for those processes that have recently occurred at other lake-terminating glaciers in southeast Iceland. Indeed, these glaciers are also underlain by deep bedrock troughs, and as a result they have undergone heightened rates of proglacial lake growth and terminus retreat over recent years, although the exact forcing mechanisms are unclear. As such, further research is required in order to better understand the complex processes driving the dynamics of lake-terminating glaciers in Iceland so that their future patterns of retreat and mass loss can be more accurately quantified.

**Supplementary Information** The online version contains supplementary material available at <https://doi.org/10.1007/s41976-025-00213-8>.

**Acknowledgements** The authors thank Eyjólfur Magnússon for sharing the bedrock topography data for Öreafajökull.

**Author Contributions** NRB, BR and JKH devised the study. NRB undertook the velocity analyses, prepared Figs. 1, 5, 6, 7, and 8, and wrote the draft version of the manuscript. AA undertook the frontal position and lake area analyses, as well as the retreat calculations, and prepared Figs. 2, 3, and 4. NRB, AA, BR, SA, KM and JKH all contributed to the writing and editing of the final manuscript.

**Funding** This research was funded by The Leverhulme Trust, grant number RPG-2021–316.

**Data Availability** The datasets generated for this study can be found in the following online repository: <https://doi.org/10.5281/zenodo.13142806>.

## Declarations

**Conflict of Interest** The authors declare no competing interests.

**Open Access** This article is licensed under a Creative Commons Attribution 4.0 International License, which permits use, sharing, adaptation, distribution and reproduction in any medium or format, as long as you give appropriate credit to the original author(s) and the source, provide a link to the Creative Commons licence, and indicate if changes were made. The images or other third party material in this article are included in the article's Creative Commons licence, unless indicated otherwise in a credit line to the material. If material is not included in the article's Creative Commons licence and your intended use is not permitted by statutory regulation or exceeds the permitted use, you will need to obtain permission directly from the copyright holder. To view a copy of this licence, visit <http://creativecommons.org/licenses/by/4.0/>.

## References

- Gardner AS, Moholdt G, Cogley JG, Wouters B, Arendt AA, Wahr J et al (2013) A reconciled estimate of glacier contributions to sea level rise: 2003 to 2009. *Science* 340(6134):852–857. <https://doi.org/10.1126/science.1234532>
- Marzeion B, Hock R, Anderson B, Bliss A, Champollion N, Fujita K et al (2020) Partitioning the uncertainty of ensemble projections of global glacier mass change. *Earth's Future* 8(7):e2019EF001470. <https://doi.org/10.1029/2019EF001470>
- Zemp M, Huss M, Thibert E, Eckert N, McNabb R, Huber J et al (2019) Global glacier mass changes and their contributions to sea-level rise from 1961 to 2016. *Nature* 568(7752):382–386. <https://doi.org/10.1038/s41586-019-1071-0>
- Farinotti D, Huss M, Fürst JJ, Landmann J, Machguth H, Maussion F et al (2019) A consensus estimate for the ice thickness distribution of all glaciers on Earth. *Nat Geosci* 12(3):168–173. <https://doi.org/10.1038/s41561-019-0300-3>
- Hugonnet R, McNabb R, Berthier E, Menounos B, Nuth C, Girod L et al (2021) Accelerated global glacier mass loss in the early twenty-first century. *Nature* 592(7856):726–731. <https://doi.org/10.1038/s41586-021-03436-z>
- Wouters B, Gardner AS, Moholdt G (2019) Global glacier mass loss during the GRACE satellite mission (2002–2016). *Front Earth Sci* 7:96. <https://doi.org/10.3389/feart.2019.00096>
- Gärtner-Roer I, Nussbaumer SU, Hüsler F, Zemp M (2019) World-wide assessment of national glacier monitoring and future perspectives. *Mt Res Dev* 39(2):A1–A11. <https://doi.org/10.1659/MRD-JOURNAL-D-19-00021.1>
- Huss M, Hock R (2018) Global-scale hydrological response to future glacier mass loss. *Nat Clim Chang* 8(2):135–140. <https://doi.org/10.1038/s41558-017-0049-x>
- Paul F, Bolch T, Kääb A, Nagler T, Nuth C, Scharrer K et al (2015) The glaciers climate change initiative: Methods for creating glacier area, elevation change and velocity products. *Remote Sens Environ* 162:408–426. <https://doi.org/10.1016/j.rse.2013.07.043>
- Björnsson H, Pálsson F, Guðmundsson S, Magnússon E, Adalgeirsdóttir G, Jóhannesson T et al (2013) Contribution of Icelandic ice caps to sea level rise: Trends and variability since the Little Ice Age. *Geophys Res Lett* 40(8):1546–1550. <https://doi.org/10.1002/grl.50278>
- Kavan J, Stuchlík R, Carrivick JL, Hanáček M, Stringer CD, Roman M, Holuša J, Dagsson-Waldhauserova P, Láska K, Nývlt D (2024) Proglacial lake evolution coincident with glacier dynamics in the frontal zone of Kviárjökull, South-East Iceland. *Earth Surf Proc Land* 49(5):1–16. <https://doi.org/10.1002/esp.5781>
- Noël B, Aðalgeirsdóttir G, Pálsson F, Wouters B, Lhermitte S, Haacker JM, van den Broeke MR (2022) North Atlantic cooling is slowing down mass loss of Icelandic glaciers. *Geophys Res Lett* 49(3):e2021GL095697. <https://doi.org/10.1029/2021GL095697>
- Foresta L, Gourmelen N, Pálsson F, Nienow P, Björnsson H, Shepherd A (2016) Surface elevation change and mass balance of Icelandic ice caps derived from swath mode CryoSat-2 altimetry. *Geophys Res Lett* 43(23):12–138. <https://doi.org/10.1002/2016GL071485>
- Aðalgeirsdóttir G, Magnússon E, Pálsson F, Thorsteinsson T, Belart J, Jóhannesson T, et al (2020) Glacier changes in Iceland from ~1890 to 2019. *Front Earth Sci* 8(520). <https://doi.org/10.3389/feart.2020.523646>
- Meredith M, Sommerkorn M, Cassotta S, Derksen C, Ekaykin A, Hollowed A, Kofinas G, Mackintosh A, Melbourne-Thomas J, Muelbert MMC, Ottersen G, Pritchard H, Schuur EAG (2019) Polar regions. In: IPCC special report on the ocean and cryosphere in a changing climate. Pörtner HO, Roberts DC, Masson-Delmotte V, Zhai P, Tignor M, Poloczanska E, Mintenbeck K, Alegria A, Nicolai M, Okem A, Petzold J, Rama B, Weyer NM (eds). Cambridge University Press, Cambridge, UK and New York, NY, USA, pp 203–320. <https://doi.org/10.1017/9781009157964.005>
- Gunnarsson A, Gardarsson SM, Pálsson F, Jóhannesson T, Sveinsson ÓGB (2021) Annual and interannual variability and trends of albedo for Icelandic glaciers. *Cryosphere* 15(2):547–570. <https://doi.org/10.5194/tc-15-547-2021>
- Jóhannesson T, Pálmason B, Hjartarson Á, Jarosch AH, Magnússon E, Belart JM et al (2020) Non-surface mass balance of glaciers in Iceland. *J Glaciol* 66(258):685–697. <https://doi.org/10.1017/jog.2020.37>
- Möller R, Dagsson-Waldhauserova P, Möller M, Kukla P, Schneider C, Guðmundsson MT (2019) Persistent albedo reduction on southern Icelandic glaciers due to ashfall from the 2010 Eyjafjallajökull eruption. *Remote Sens Environ* 233:111396. <https://doi.org/10.1016/j.rse.2019.111396>
- Benn DI, Warren CR, Mottram RH (2007) Calving processes and the dynamics of calving glaciers. *Earth Sci Rev* 82(3–4):143–179. <https://doi.org/10.1016/j.earscirev.2007.02.002>
- Carrivick JL, Tweed FS (2013) Proglacial lakes: Character, behaviour and geological importance. *Quatern Sci Rev* 78:34–52. <https://doi.org/10.1016/j.quascirev.2013.07.028>
- Truffer M, Motyka RJ (2016) Where glaciers meet water: Subaqueous melt and its relevance to glaciers in various settings. *Rev Geophys* 54(1):220–239. <https://doi.org/10.1002/2015RG000494>
- Guðmundsson S, Björnsson H, Pálsson F, Magnússon E, Sæmundsson P, Jóhannesson T (2019) Terminus lakes on the south side of Vatnajökull ice cap, SE-Iceland. *Jökull* 69:1–34
- Magnússon E, Pálsson F, Björnsson H, Guðmundsson S (2012) Removing the ice cap of Öræfajökull central volcano, SE Iceland: mapping and interpretation of bedrock topography, ice volumes, subglacial troughs and implications for hazards assessments. *Jökull* 62:131–150
- Dell R, Carr R, Phillips E, Russell AJ (2019) Response of glacier flow and structure to proglacial lake development and climate

- at Fjallsjökull, south-east Iceland. *J Glaciol* 65(250):321–336. <https://doi.org/10.1017/jog.2019.18>
25. Hannesdóttir H, Björnsson H, Pálsson F, Aðalgeirsdóttir G, Guðmundsson S (2015) Changes in the southeast Vatnajökull ice cap, Iceland, between~ 1890 and 2010. *Cryosphere* 9(2):565–585. <https://doi.org/10.5194/tc-9-565-2015>
  26. Schomacker A (2010) Expansion of ice-marginal lakes at the Vatnajökull ice cap, Iceland, from 1999 to 2009. *Geomorphology* 119(3–4):232–236. <https://doi.org/10.1016/j.geomorph.2010.03.022>
  27. Voytenko D, Dixon TH, Howat IM, Gourmelen N, Lembke C, Werner CL, de la Peña S, Oddsson B (2015) Multi-year observations of Breiðamerkurjökull, a marine-terminating glacier in southeastern Iceland, using terrestrial radar interferometry. *J Glaciol* 61(225):42–54. <https://doi.org/10.3189/2015JoG14J099>
  28. Guðmundsson S, Björnsson H (2016) Changes in the flow pattern of Breiðamerkurjökull reflected by bending of the Esjufjallaronð medial moraine. *Jökull* 66:95–100
  29. Storrar RD, Jones AH, Evans DJ (2017) Small-scale topographically-controlled glacier flow switching in an expanding proglacial lake at Breiðamerkurjökull, SE Iceland. *J Glaciol* 63(240):745–750. <https://doi.org/10.1017/jog.2017.22>
  30. Baurley NR, Robson BA, Hart JK (2020) Long-term impact of the proglacial lake Jökulsárlón on the flow velocity and stability of Breiðamerkurjökull glacier, Iceland. *Earth Surf Processes Landf* 45(11):2647–2663. <https://doi.org/10.1002/esp.4920>
  31. Baurley NR (2022) Insights into the seasonal dynamics of the lake-terminating glacier Fjallsjökull, south-east Iceland, inferred using ultra-high resolution repeat UAV imagery. Doctoral thesis, University of Southampton. Retrieved from: <https://eprints.soton.ac.uk/471220/>. Accessed 6 Mar 2024
  32. Baurley NR, Hart JK (2024) The role of thermal notch erosion in forcing localised calving failure and short-term increases in velocity at a lake-terminating glacier in southeast Iceland. *Eartharxiv* [Preprint]. <https://doi.org/10.31223/X58D82>
  33. Guðmundsson S, Björnsson H, Pálsson F (2017) Changes of Breiðamerkurjökull glacier, SE-Iceland, from its late nineteenth century maximum to the present. *Geogr Ann Ser B* 99(4):338–352. <https://doi.org/10.1080/04353676.2017.1355216>
  34. Evans DJ, Twigg DR (2002) The active temperate glacial landsystem: A model based on Breiðamerkurjökull and Fjallsjökull, Iceland. *Quat Sci Rev* 21(20–22):2143–2177. [https://doi.org/10.1016/S0277-3791\(02\)00019-7](https://doi.org/10.1016/S0277-3791(02)00019-7)
  35. Björnsson H (1996) Scales and rates of glacial sediment removal: A 20 km long, 300 m deep trench created beneath Breiðamerkurjökull during the Little Ice Age. *Ann Glaciol* 22:141–146. <https://doi.org/10.3189/1996AoG22-1-141-146>
  36. Dehecq A, Gourmelen N, Trouvé E (2015) Deriving large-scale glacier velocities from a complete satellite archive: Application to the Pamir–Karakoram–Himalaya. *Remote Sens Environ* 162:55–66. <https://doi.org/10.1016/j.rse.2015.01.031>
  37. Fahnestock M, Scambos T, Moon T, Gardner A, Haran T, Klinger M (2016) Rapid large-area mapping of ice flow using Landsat 8. *Remote Sens Environ* 185:84–94. <https://doi.org/10.1016/j.rse.2015.11.023>
  38. Nagler T, Rott H, Hetzenecker M, Wuite J, Potin P (2015) The Sentinel-1 mission: New opportunities for ice sheet observations. *Remote Sens* 7(7):9371–9389. <https://doi.org/10.3390/rs70709371>
  39. Lal P, Vaka DS, Rao YS (2018) Mapping Surface Flow Velocities of Siachen and Gangotri Glaciers Using Terrasar-X and SENTINEL-1A Data by Intensity Tracking. *ISPRS Ann Photogramm Remote Sens Spat Inform Sci* 4:325–329
  40. Yang R, Hock R, Kang S, Guo W, Shangguan D, Jiang Z et al (2022) Glacier surface speed variations on the Kenai Peninsula, Alaska, 2014–2019. *J Geophys Res Earth Surf* 127(3):e2022JF006599. <https://doi.org/10.1029/2022JF006599>
  41. Landmælingar Íslands (2016) National Land Survey of Iceland – LiDAR DEM of Iceland. Retrieved from: <https://gatt.lmi.is/geonetwork/srv/eng/catalog.search#/metadata/cb84d208-1b91-4b9e-a21c-93c4e284f488>. Accessed 1 Sept 2023
  42. Robson BA, Nuth C, Nielsen PR, Girod L, Hendrickx M, Dahl SO (2018) Spatial variability in patterns of glacier change across the Manaslu Range, Central Himalaya. *Front Earth Sci* 6:12. <https://doi.org/10.3389/feart.2018.00012>
  43. Moon T, Joughin I (2008) Changes in ice front position on Greenland's outlet glaciers from 1992 to 2007. *J Geophys Res Earth Surf* 113(F2). <https://doi.org/10.1029/2007JF000927>
  44. Larsen SH, Khan SA, Ahlström AP, Hvidberg CS, Willis MJ, Andersen SB (2016) Increased mass loss and asynchronous behaviour of marine-terminating outlet glaciers at Upernavik Isstrøm, NW Greenland. *J Geophys Res Earth Surf* 121(2):241–256. <https://doi.org/10.1002/2015JF003507>
  45. Lea JM, Mair DW, Rea BR (2014) Evaluation of existing and new methods of tracking glacier terminus change. *J Glaciol* 60(220):323–332. <https://doi.org/10.3189/2014JoG13J061>
  46. Wuite J, Libert L, Nagler T, Jóhannesson T (2022) Continuous monitoring of ice dynamics in Iceland with Sentinel-1 satellite radar images. *Jökull* 72(1):1–20. <https://doi.org/10.33799/jokul12021.72.001>
  47. Gardner AS, Fahnestock MA, Scambos TA (2024) (accessed 10<sup>th</sup> February 2024). ITS\_LIVE Regional Glacier and Ice Sheet Surface Velocities. Data archived at National Snow and Ice Data Center. <https://doi.org/10.5067/6II6VW8LLWJ7>
  48. Rohner C, Small D, Beutel J, Henke D, Lüthi MP, Vieli A (2019) Multisensor validation of tidewater glacier flow fields derived from synthetic aperture radar (SAR) intensity tracking. *Cryosphere* 13:2953–2975. <https://doi.org/10.5194/tc-13-2953-2019>
  49. Altena B, Käb A (2017) Weekly glacier flow estimation from dense satellite time series using adapted optical flow technology. *Front Earth Sci* 5:1–12. <https://doi.org/10.3389/feart.2017.00053>
  50. Joughin I, Smith BE, Howat I (2018) Greenland Ice Mapping Project: Ice Flow Velocity Variation at sub-monthly to decadal time scales. *Cryosphere* 12(7):2211–2227. <https://doi.org/10.5194/tc-12-2211-2018>
  51. Millan R, Mougnot J, Rabatel A, Jeong S, Cusicanqui D, Derkacheva A, Chekki M (2019) Mapping surface flow velocity of glaciers at regional scale using a multiple sensors approach. *Remote Sensing* 11(21):2498. <https://doi.org/10.3390/rs11212498>
  52. Friedl P, Seehaus T, Braun M (2021) Global time series and temporal mosaics of glacier surface velocities derived from Sentinel-1 data. *Earth Syst Sci Data* 13:4653–4675. <https://doi.org/10.5194/essd-13-4653-2021>
  53. Sugiyama S, Sakakibara D, Tsutaki S, Maruyama M, Sawagaki T (2015) Glacier dynamics near the calving front of Bowdoin Glacier, northeastern Greenland. *J Glaciol* 61(226):223–232. <https://doi.org/10.3189/2015JoG14J127>
  54. Sugiyama S, Skvarca P, Naito N, Enomoto H, Tsutaki S, Tone K, Marinsek S, Aniya M (2011) Ice speed of a calving glacier modulated by small fluctuations in basal water pressure. *Nat Geosci* 4(9):597–600. <https://doi.org/10.1038/ngeo1218>
  55. Trüssel BL, Motyka RJ, Truffer M, Larsen CF (2013) Rapid thinning of lake-calving Yakutat Glacier and the collapse of the Yakutat Icefield, southeast Alaska, USA. *J Glaciol* 59(213):149–161. <https://doi.org/10.3189/2013JOG12J081>
  56. Tsutaki S, Sugiyama S, Nishimura D, Funk M (2013) Acceleration and flotation of a glacier terminus during formation of a proglacial lake in Rhonegletscher, Switzerland. *J Glaciol* 59(215):559–570. <https://doi.org/10.3189/2013JoG12J107>

57. Tsutaki S, Fujita K, Nuimura T, Sakai A, Sugiyama S, Komori J, Tshering P (2019) Contrasting thinning patterns between lake- and land-terminating glaciers in the Bhutanese Himalaya. *Cryosphere* 13(10):2733–2750. <https://doi.org/10.5194/tc-13-2733-2019>
58. King O, Dehecq A, Quincey D, Carrivick J (2018) Contrasting geometric and dynamic evolution of lake and land-terminating glaciers in the central Himalaya. *Global Planet Change* 167:46–60. <https://doi.org/10.1016/j.gloplacha.2018.05.006>
59. Minowa M, Schaefer M, Skvarca P (2023) Effects of topography on dynamics and mass loss of lake-terminating glaciers in southern Patagonia. *J Glaciol*: 1–18. <https://doi.org/10.1017/jog.2023.42>
60. Liu Q, Mayer C, Wang X, Nie Y, Wu K, Wei J, Liu S (2020) Interannual flow dynamics driven by frontal retreat of a lake-terminating glacier in the Chinese Central Himalaya. *Earth Planet Sci Lett* 546:116450. <https://doi.org/10.1016/j.epsl.2020.116450>
61. Catania GA, Stearns LA, Sutherland DA, Fried MJ, Bartholomaeus TC, Morlighem M, Shroyer E, Nash J (2018) Geometric controls on tidewater glacier retreat in central western Greenland. *J Geophys Res Earth Surf* 123:2024–2038. <https://doi.org/10.1029/2017JF004499>
62. Pronk JB, Bolch T, King O, Wouters B, Benn DI (2021) Contrasting surface velocities between lake- and land-terminating glaciers in the Himalayan region. *Cryosphere* 15:5577–5599. <https://doi.org/10.5194/tc-15-5577-2021>
63. Nick FM, van der Kwast J, Oerlemans J (2007) Simulation of the evolution of Breiðamerkurjökull in the late Holocene. *J Geophys Res Solid Earth* 112(B1). <https://doi.org/10.1029/2006JB004358>
64. Flowers GE, Marshall SJ, Björnsson H, Clarke GK (2005) Sensitivity of Vatnajökull ice cap hydrology and dynamics to climate warming over the next 2 centuries. *J Geophys Res Earth Surf* 110(F2). <https://doi.org/10.1029/2004JF000200>
65. Schmidt LS, Adalgeirsdóttir G, Pálsson F, Langen PL, Guðmundsson S, Björnsson H (2019) Dynamic simulations of Vatnajökull ice cap from 1980 to 2300. *J Glaciol* 66(255):97–112. <https://doi.org/10.1017/jog.2019.90>
66. Bennett GL, Evans DJA (2012) Glacier retreat and landform production on an overdeepened glacier foreland: the debris-charged glacial landsystem at Kvíárjökull, Iceland. *Earth Surface Process and Landforms* 37:1584–1602. <https://doi.org/10.1002/esp.3259>
67. Phillips E, Everest J, Evans DJA, Finlayson A, Ewertowski M, Guild A, Jones L (2017) Concentrated, ‘pulsed’ axial glacier flow: structural glaciological evidence from Kvíárjökull in SE Iceland. *Earth Surf Proc Land* 42(13):1901–1922. <https://doi.org/10.1002/esp.4145>
68. Nicholson L, Benn DI (2013) Properties of natural supraglacial debris in relation to modelling sub-debris ice ablation. *Earth Surf Proc Land* 38(5):490–501. <https://doi.org/10.1002/esp.3299>
69. Reznichenko N, Davies T, Shulmeister J, McSaveney M (2010) Effects of debris on ice-surface melting rates: an experimental study. *J Glaciol* 56(197):384–394. <https://doi.org/10.3189/002214310792447725>
70. Carrivick JL, Tweed FS, Sutherland JL, Mallalieu J (2020) Toward numerical modelling of interactions between ice-marginal proglacial lakes and glaciers. *Front Earth Sci* 8:500. <https://doi.org/10.3389/feart.2020.577068>
71. Boyce ES, Motyka RJ, Truffer M (2007) Flotation and retreat of a lake-calving terminus, Mendenhall Glacier, southeast Alaska, USA. *J Glaciol* 53(181):211–224. <https://doi.org/10.3189/172756507782202928>
72. Adhikari S, Marshall SJ (2012) Parameterization of lateral drag in flowline models of glacier dynamics. *J Glaciol* 58(212):1119–1132. <https://doi.org/10.3189/2012JG12J018>
73. Dehecq A, Gourmelen N, Gardner AS, Brun F, Goldberg D, Nienow PW, Berthier E, Vincent C, Wagnon P, Trouvé E (2019) Twenty-first century glacier slowdown driven by mass loss in High Mountain Asia. *Nat Geosci* 12(1):22–27. <https://doi.org/10.1038/s41561-018-0271-9>
74. Sato Y, Fujita K, Inoue H, Sakai A, Karma (2022) Land-to lake-terminating transition triggers dynamic thinning of a Bhutanese glacier. *The Cryosphere* 16(6):2643–2654. <https://doi.org/10.5194/tc-16-2643-2022>
75. Warren C, Benn D, Winchester V, Harrison S (2001) Buoyancy-driven lacustrine calving, Glaciar Nef, Chilean Patagonia. *J Glaciol* 47(156):135–146. <https://doi.org/10.3189/172756501781832403>
76. Motyka RJ, O’Neel S, Connor CL, Echelmeyer KA (2003) Twentieth century thinning of Mendenhall Glacier, Alaska, and its relationship to climate, lake calving, and glacier run-off. *Global Planet Change* 35(1–2):93–112. [https://doi.org/10.1016/S0921-8181\(02\)00138-8](https://doi.org/10.1016/S0921-8181(02)00138-8)
77. Röhl K (2006) Thermo-erosional notch development at fresh-water-calving Tasman Glacier, New Zealand. *J Glaciol* 52(177):203–213. <https://doi.org/10.3189/172756506781828773>
78. Ben-Yehoshua D, Sæmundsson Þ, Helgason JK, Belart JMC, Sigurðsson JV, Erlingsson S (2022) Paraglacial exposure and collapse of glacial sediment: the 2013 landslide onto Svínafellsjökull, southeast Iceland. *Earth Surf Proc Land* 47(10):2612–2627. <https://doi.org/10.1002/esp.5398>
79. Fyffe CL, Woodget AS, Kirkbride MP, Deline P, Westoby MJ, Brock BW (2020) Processes at the margins of supraglacial debris cover: Quantifying dirty ice ablation and debris redistribution. *Earth Surf Proc Land* 45(10):2272–2290. <https://doi.org/10.1002/esp.4879>
80. Sakakibara D, Sugiyama S, Sawagaki T, Marinsek S, Skvarca P (2013) Rapid retreat, acceleration and thinning of Glaciar Upsala, Southern Patagonia Icefield, initiated in 2008. *Ann Glaciol* 54(63):131–138. <https://doi.org/10.3189/2013AoG63A236>

**Publisher's Note** Springer Nature remains neutral with regard to jurisdictional claims in published maps and institutional affiliations.